MASTERARBEIT / MASTER'S THESIS

Titel der Masterarbeit / Title of the Master's Thesis

"CO_2 fluxes of four different plant compositions in the Püergschachen Moor in the Styrian Enns valley, Austria"

verfasst von / submitted by

Asaad Saad, BSc

angestrebter akademischer Grad / in partial fulfilment of the requirements for the degree of

Master of Science (MSc)

Wien, 2017 / Vienna 2017

Studienkennzahl lt. Studienblatt / degree programme code as it appears on the student record sheet:	A 066 299
Studienrichtung lt. Studienblatt / degree programme as it appears on the student record sheet:	Interdisziplinäres Masterstudium Environmental Sciences
Betreut von / Supervisor:	Univ.-Prof. Dipl.-Geogr. Dr. Stephan Glatzel

ABSTRACT

Peatlands cover over four million km^2 representing 3% of the land and freshwater surface of the planet and contains one third of the world's soil carbon. In this study, CO_2 exchange fluxes were measured in four sites located in Püergschachen Moor in the Styrian Enns valley, Austria representing four different plant compositions in the study area. Measurements were done during spring, summer and autumn using closed dynamic chamber approach and gas measurements were made using infrared gas analyser. The seasonal variability in addition to changes over day time of ecosystem respiration (R_{eco}), gross primary production (GPP) and net ecosystem exchange (NEE) were investigated with respect to photosynthetic active radiation (PAR) and soil temperature measured at 2cm depth, water table changes were also considered. The effect of the different plant composition in the four sites on R_{eco}, GPP and NEE were investigated. Finally, R_{eco}, GPP and NEE were modelled and estimated fluxes were calculated in order to calculate the total CO_2 exchange per square meter for the ecosystem over the year.

In the study, R_{eco} showed strong positive correlation with temperature changes over the day time and seasonal variabilities. On the other hand, respiration had low correlation with water table. GPP increased with PAR increase following the plant photosynthesis light response curve. NEE at low PAR values showed CO_2 release and with PAR increase production increase leading to CO_2 uptake by the system. Warmer seasons showed higher production fluxes, indicating that PAR was not the only factor affecting GPP and temperature plays a role as well.

Model results indicated sites PM2 and PM4 "*Pinus mugo*" (PM4 plants are larger than PM2) are showing CO_2 release (annual NEE amounts +1.227 kg m^{-2} y^{-1} in PM2); while PM3 "*Calluna vulgaris*" showed CO_2 uptake (annual NEE amounts -1.129 kg m^{-2} y^{-1}) and PM1 "*Eriophorum vaginatum & Rhynchospora alba*" showed low NEE fluxes. The highest annual GPP was in PM3 (-3.854 kg m^{-2} y^{-1}) and the highest annual R_{eco} was in PM2 (3.761 kg m^{-2} y^{-1}). These results suggest that the distribution of plant composition and size has a significant role in the peatland and is an influencing parameter in carbon exchange within this ecosystem, and affecting its status as a CO_2 sink or source.

Keywords: peatland - ecosystem respiration - gross primary production - net ecosystem exchange - plant composition

ABSTRAKT

Moore bedecken ca. 3% der Land- und Süßwasseroberfläche der Erde, was über über vier Millionen km^2 entspricht. Sie enthalten ein Drittel des weltweiten Bodenkohlenstoffs. Im Pürgschachen-Moor im Ennstal (Steiermark, Österreich) kommen vier verschiedene Pflanzenzusammensetzungen vor, an denen im Zuge dieser Studie CO_2-Austauschflüsse gemessen wurden. Im Frühjahr, Sommer und Herbst wurden Probennahmen und Messungen mit der geschlossenen dynamischen Haubenmessmethode und Infrarot-Gasanalysatoren durchgeführt. Untersucht wurden jahres- und tageszeitliche Änderungen der Ökosystemrespiration (ecosystem respiration - R_{eco}), Bruttoprimärproduktion (gross primary production - GPP) und des Netto-Ökosystemaustauschs (net ecosystem exchange - NEE) wurden über die photosynthetisch aktive Strahlung (PAR) und Bodentemperatur in 2 cm Tiefe gemessen, wobei auch Grundwasserspiegelschwankungen berücksichtigt wurden. Untersucht wurde die Wirkung der verschiedenen Pflanzenzusammensetzungen der vier Standorte auf R_{eco}, GPP und NEE. Schließlich wurden R_{eco}, GPP und NEE modelliert, um mit den Schätzungen der Flüsse den Gesamt-CO_2-Austausch pro Quadratmeter für das Ökosystem über das Jahr zu berechnen.

Einerseits zeigte R_{eco} in der Studie eine starke positive Korrelation mit Temperaturänderungen über die Tageszeit und saisonalen Unterschieden, andererseits war die Korrelation zwischenRespirationund Grundwasserspiegel gering. GPP stieg mit PAR-Zunahme in Übereinstimmung mit der Lichtsättigungskurve. NEE zeite bei niedrigen PAR-Werten CO_2-Freisetzung und bei PAR-Zunahme herhöhte Produktion und dadurch CO_2-Aufnahme durch das System. Wärmere Jahreszeiten zeigten höhere Produktionsflüsse, was darauf hinweist, dass PAR nicht der einzige Faktor war, der das GPP beeinflusst, sondern auch Temperatur eine Rolle spielt.

Laut Modell zeigen Standorte PM2 und PM4 "Pinus mugo" (Pflanzen in PM4 sind größer als PM2) CO_2-Freisetzung (jährliche NEE-Beträge +1.227 kg m^{-2} y^{-1} in PM2), während PM3 "Calluna vulgaris" CO_2-Aufnahme zeigt (jährliche NEE betrug -1.129 kg m^{-2} y^{-1}) und PM1 "Eriophorum vaginatum & Rhynchospora alba" niedrige NEE-Flüsse zeigen. Die höchste jährliche GPP befand sich in PM3 (-3.854 kg m^{-2} y^{-1}) und der höchste jährliche R_{eco} in PM2 (3.761 kg m^{-2} y^{-1}). Diese Resultate legen nahe, dass die Verteilung der Pflanzenzusammensetzung und die Größe der Pflanzen eine bedeutende Rolle in Mooren spielen und den Kohlenstoffaustausch innerhalb des Ökosystems als Parameter beeinflussen, und dadurch auch Einfluss auf den Status des Ökosystems als CO_2-Senke oder Quelle haben.

Schlüsselwörter: Moore - Ökosystemrespiration - Bruttoprimärproduktion - Netto-Ökosystem-Austausch - Pflanzenzusammensetzung

ACKNOWLEDGMENTS

I would first like to thank my thesis supervisor Univ.-Prof. Dipl.-Geogr. Dr. Stephan Glatzel for his guidance, support and answer all my queries. Also, special thanks to Simon Drollinger MSc, who read my numerous revisions and helped sort some of the challenges during the full process of taking readings, analysing and reaching a conclusion. He consistently allowed this thesis to be my own work, but steered me in the right the direction whenever he thought I needed it. And finally, thanks to my wife, daughters and friends who endured this long process with me, always offering support and love.

CURRICULUM VITA

Name	: Asaad Nabil Asaad
Family name	: Saad
Date of birth	: Jan. 14th, 1968.
Place of birth	: Cairo
Marital Status	: Married with two Children
Nationality	: Egyptian
Address	: Saied Zakaria St. (Bldg. 19 Block 6), El-Sefarat District, Nasr City, Cairo, Egypt.
Mobil	: +20 100 171 6631
E-mail	: asaad.nabil@hotmail.com

1. Qualifications

- **Membership of Professional / Occupational Institutions:**
  - Member in Egyptian Engineers Syndicate
  - MCIArb. – Member in the Chartered Institute of Arbitrators (CIArb), London England
  - MCIArb. – Member in the Chartered Institute of Arbitrators (CIArb), Cairo Branch
  - Member in Egyptian Engineers Society
  - Member in the Contracts Committee assigned by the Ministerial Decree for the preparation of the Egyptian Code of Project Management (2008)
- **Language Skills:**

Mother language: Arabic

	Speaking	Writing
English	V. Good	V. Good
German	Fair	Fair

- **Education:**

Present time	M.Sc. Environmental Sciences –University of Vienna
June 2008	Law Degree – Faculty of Law - Ain Shams University
April 2003	Ph.D. Civil Engineering “Comparative Study between FIDIC’s Contract Conditions for Civil Construction 4th edition and FIDIC’s Contract Conditions for Construction 1999 issue” Faculty of Engineering - Ain Shams University.

April 1997 M.Sc. Civil Engineering (Structure)
"Structural Analysis of Offshore Pipelines"
Faculty of Engineering - Ain Shams University.

July 1990 B.Sc. Civil Engineering (Structure) degree "V. Good with Honor"
(Steel Structures Project) degree "V. Good"

- **Computer Qualifications:**
  - Very Good knowledge with MS Office applications
  - Knowledge of geochemical modelling using PHREEQC Interactive
  - Knowledge of statistical analysis using R
  - Knowledge of groundwater modelling using MODFLOW
  - Knowledge of digital maps and GIS using ArcGIS
  - Capable of dealing with any software easily and efficiently

2. Work History

- **From September 2016 to Present Time:**

Organization : Ministry of Planning, General Secretariat of the Supreme Council for Planning and Development (GSSCPD), State of Kuwait

Position : Engineering Projects Tendering Specialist (Consultants Department)

- **From February 2008 to June 2015:**

Institution : American University in Cairo (AUC)

Position **:** Instructor and since March 2014 Associate Professor (on part time basis)

- **From November 2010 to January 2015:**

Company : Al Amar Consulting Group S.A., Cairo, Egypt

Position : Vice President - Head of Business Development Division, Manager of Corporate Planning Department and Technical Office Department as well as Projects Manager

- **From December 2009 to November 2010:**

Company : ENI Oil Co. Ltd. - Libyan Branch (currently named Mellitah Oil & Gas B.V. - Libyan Branch)

The assignment was made through "First Engineering & Software Systems" on indirect hiring basis.

Position : Contracts Specialist

- **From August 1998 to November 2009:**

Company : ECG Engineering Consultants Group S.A.

Position : From January 2009 to November 2009 “Contracts & Follow-up – Department Manager”

: From March 2006 to December 2008 “Assistant President & Contracts Manager”

Position : From August 1998 to February 2006 “Specifications & Contracts Writer” – Department Manager from June 2004

- **From April 2002 to October 2002:**

Company : Burullus Gas Company (a subsidiary to Rashid Petroleum Company) - Scarab/Saffron Development Project)

The assignment was made through “First Egyptian Co. for Engineering” on indirect hiring basis.

Position : Contracts Engineer

- **From December 1997 to June 1998:**

Company : Kuwait National Petroleum Company (KNPC)

The assignment was made through “Heston (Middle East) LTD.” on indirect hiring basis.

Position : Contracts Engineer

- **From January 1991 to December 1997:**

Company : Petroleum Projects and Technical Consultation Co. “PETROJET”

Position : From August 1993 to December 1997 “Contracts Engineer”

: From January 1991 to August 1993 “Offshore Engineer, Offshore Engineering office”

- **From August 1990 to January 1991:**

Company : “W.D.O.” - Wassif Design Office

Position : Design Engineer (Design of civil Structures)

Table of Contents

ABSTRACT 2

ABSTRAKT 3

ACKNOWLEDGMENTS 4

CURRICULUM VITA 5

LIST OF FIGURES iv

LIST OF TABLES v

LIST OF ABBREVIATIONS vi

CHAPTER 1 – INTRODUCTION 1

1.1 General 1

1.2 Peatlands in Brief 1

1.2.1 Peatlands Definition 1

1.2.2 Peatlands Distribution 2

1.3 Peatlands and Carbon Cycle 2

1.3.1 Photosynthesis & Respiration 2

1.3.2 Peatland Profile (Matrix) 3

1.3.3 Carbon Cycle in Peatlands 3

1.3.4 Peatlands as a Carbon Sink 4

1.3.5 Peatlands Degradation 5

1.4 Aim of this Study 5

1.4.1 Methodology 6

CHAPTER 2 - FIELD MEASUREMENTS 7

2.1 Study Area 7

2.1.1 Background 7

2.1.2 Sites and Frames 7

2.2 CO_2 Measurement Approaches 9

2.2.1 Eddy Covariance Approach 9

2.2.2 Closed Chamber Approach 11

2.2.3 Approach Used 12

2.3 Instruments and Tools Used 12

2.3.1 Chamber Frames 12

2.3.2 Closed Dynamic Chambers 13

2.3.3 Infra-Red Gas Analyser (IRGA) 13

2.4 Measured Data 14

2.4.1 Measurement Plan 14

2.4.2 GERD Measurements 15
2.5 CO_2 Flux Calculations 16
2.5.1 Methodology 16
2.5.2 Calculated CO_2 Fluxes 17
CHAPTER 3 - RESULTS 19
3.1 Data Grouping 19
3.2 Seasonal Variability 20
3.2.1 CO_2 Fluxes Distribution with Respect to PAR 20
3.2.2 CO_2 Fluxes Distribution with Respect to Soil Temperature 21
3.2.3 CO_2 Fluxes Distribution with Respect to Day Time 23
3.2.4 Seasonal Variability Summary 26
3.3 Comparison between the Four Sites 27
3.3.1 PAR Categorization 27
3.3.2 Soil Temperature Categorization 30
3.3.3 Comparison the Four Sites Summary 33
3.4 Comparison within the Site 35
3.4.1 Site PM1 Frames 35
3.4.2 Site PM2 Frames 36
3.4.3 Site PM3 Frames 36
3.4.4 Site PM4 Frames 37
3.5 Eddy Covariance Results Comparison 37
3.6 CO_2 Balance for the Ecosystem 38
3.6.1 Soil and Air Temperature Correlation 38
3.6.2 Ecosystem Respiration (R_{eco}) 39
3.6.3 Net Ecosystem Exchange (NEE) 40
3.6.4 Ecosystem CO_2 Balance 41
CHAPTER 4 – DISCUSSION 44
4.1 Ecosystem Respiration (R_{eco}) 44
4.1.1 Seasonal Variability 44
4.1.2 Water Table Dependency 44
4.1.3 Temperature Dependency 45
4.2 Gross Primary Production (GPP) 46
4.2.1 Seasonal Variability 46
4.2.2 PAR Dependency 46
4.2.3 Temperature Dependency 46
4.3 Net Ecosystem Exchange (NEE) 47

4.3.1 Day-time NEE 47
4.3.2 Total NEE 47
4.3.3 Plant Composition 48
CHAPTER 5 - CONCLUSIONS 50
REFERENCES 52
ANNEXES 54
Annex 1 – CO_2 Fluxes Calculations' R-Script 54
Annex 2 – Sites' Frames Results 59
Annex 3 – NEE and R_{eco} Models 60

LIST OF FIGURES

Figure 1: Fens and Bogs 1
Figure 2: Distribution of Mires (Source IPS “International Peat Society”) 2
Figure 3: Processes inside Peatlands 4
Figure 4: Püergschachen Moor (source: www.moor.ardning.at) 7
Figure 5: Sites and Frames Distribution in Study Area 8
Figure 6: The three Frames in Site PM1 8
Figure 7: The three Frames in Site PM2 8
Figure 8: The three Frames in Site PM3 9
Figure 9: The three Frames in Site PM4 9
Figure 10: Eddy Covariance Principals 9
Figure 11: Eddy Tower in Study Area 10
Figure 12: Closed Dynamic Chamber - Schematic Diagram (source: Sutitarnnontr et al., 2012) 11
Figure 13: Frame fitted in the Site 12
Figure 14: Transparent Closed Dynamic Chamber 13
Figure 15: Opaque Closed Dynamic Chamber 13
Figure 16: Radiation Adsorption by GHG (source: clivebest.com) 14
Figure 17: LI-820 "CO_2 Gas Analyser" 14
Figure 18: Sample of GERD output data 15
Figure 19: Sample Measurement - Transparent Chamber measurement session 16
Figure 20: Sample Measurement - Opaque Chamber measurement session 16
Figure 21: Distribution of NEE (g m^{-2} h^{-1}) with respect to PAR (µmol $photon^{-1}$ m^{-2} s^{-1}) 21
Figure 22: Distribution of CO_2 Fluxes (g m^{-2} h^{-1}) with respect to Soil Temperature (°C) at 2cm Depth – Transparent Chamber 22
Figure 23: Distribution of CO_2 Fluxes (g m^{-2} h^{-1}) with respect to Soil Temperature (°C) at 2cm Depth – Opaque Chamber 23
Figure 24: Day time average hourly distribution of seasonal PAR (µmol $photon^{-1}$ m^{-2} s^{-1}) and temperature (°C) 25
Figure 25: Day time average hourly distribution of seasonal CO_2 fluxes (g m^{-2} h^{-1}) 26
Figure 26: PAR Categorization and Distribution per Site (Summer Measurements) “CO_2 fluxes in (g m^{-2} h^{-1})” 28
Figure 27: PAR Categorization and Distribution per Site (Spring Measurements) “CO_2 fluxes in (g m^{-2} h^{-1})” 29
Figure 28: PAR Categorization and Distribution per Site (Autumn Measurements) “CO_2 fluxes in (g m^{-2} h^{-1})” 30
Figure 29: Soil Temp. Categorization and Distribution per Site (Summer - Transparent) “CO_2 fluxes in (g m^{-2} h^{-1})” 31
Figure 30: Soil Temp. Categorization and Distribution per Site (Summer - Opaque) “CO_2 fluxes in (g m^{-2} h^{-1})” 32
Figure 31: Temperature Correlation Matrix 39
Figure 32: Photosynthesis light response curve 46

LIST OF TABLES

Table 1: Peatland Profile (Matrix) 3
Table 2: Emissions from organic soils (CO_2 equivalents (kg/ha/y) 5
Table 3: Plant Species in Study Sites 7
Table 4: Comparison between Dynamic and Static Closed Chamber Approach 11
Table 5: Sample CO_2 Calculated Fluxes 17
Table 6: CO_2 Fluxes in other Literatures 18
Table 7: Distribution of Calculated Fluxes over Study Sites 19
Table 8: Seasonal Distribution of Calculated Fluxes - Transparent Chamber 19
Table 9: Seasonal Distribution of Calculated Fluxes - Opaque Chamber 20
Table 10: Seasonal average NEE per PAR categories 20
Table 11: Day time average hourly values of seasonal R_{eco}, NEE and GPP hourly 24
Table 12: Day time average hourly values of seasonal temperature and PAR 25
Table 13: Average NEE per site and PAR category - Summer Measurements 28
Table 14: Average NEE per site and PAR category - Spring & Autumn Measurements 29
Table 15: NEE and R_{eco} distribution per temperature category and site (Summer Measurements) 30
Table 16: NEE and R_{eco} distribution per temperature category and site (Spring & Autumn Measurements) 32
Table 17: Average water level at the four sites 33
Table 18: Calculated GPP distribution per temperature category and site (Summer Measurements) 34
Table 19: Calculated GPP distribution per temperature category and site (Spring & Autumn Measurements) 34
Table 20: Site PM1 Frames correlation coefficients 36
Table 21: Site PM2 Frames correlation coefficients 36
Table 22: Site PM3 Frames correlation coefficients 36
Table 23: Site PM4 Frames correlation coefficients 37
Table 24: Eddy Covariance results comparison 37
Table 25: Temperature Correlation Matrix 38
Table 26: Respiration model parameters 40
Table 27: NEE model parameters 41
Table 28: Estimated Sun Rise and Sun Set 41
Table 29: Seasonal and annual CO_2 balance per square meter 42
Table 30: Average seasonal NEE, day time R_{eco} and calculated GPP per Frame 59
Table 31: Average recorded measurements "from Eddy measurement station" 60
Table 32: Hourly seasonal GPP estimate (g m^{-2} h^{-1}) 62
Table 33: Hourly seasonal day time NEE estimate (g m^{-2} h^{-1}) 64
Table 34: Hourly seasonal R_{eco} estimate (g m^{-2} h^{-1}) 66

LIST OF ABBREVIATIONS

a.s.l.	above sea level
CH_4	Methane
CO_2	Carbon Dioxide
DOC	Dissolved Organic Carbon
GERD	Gas Emission Research Detector
GHG	Green House Gas
GPP	Gross Primary Production
GWP	Global Warming Potential
IRGA	Infra-Red Gas Analyser
N_2O	Nitrous oxide
NEE	Net Ecosystem Exchange
PAR	Photosynthetic Active Radiation (µmol photon^{-1} m^{-2} s^{-1})
POC	Particulate Organic Carbon
ppm	Part per Million
R_{eco}	Ecosystem Respiration

CHAPTER 1 – INTRODUCTION

1.1 General

Several ecosystems exist in the environment one of which is Peatlands. Peatlands have its specific characteristics which lead to an integrated role in the global environment of the earth. In this study the role of peatlands in the carbon cycle will be investigated in a study area to obtain better understanding which might be helpful to encourage conserving this important ecosystem and protect it from being degraded.

1.2 Peatlands in Brief

1.2.1 Peatlands Definition

Peatlands are the most widespread of all wetland types in the world (Joosten et al, 2002), representing 50 to 70% of the global wetlands. They cover over four million km^2 (Frolking S. et al, 2011) representing 3% of the land and freshwater surface of the planet. A wetland is an area either permanently saturated or covered with water frequently for duration sufficient to have an ecosystem adopted for life in saturated soil conditions. As will be explained later, peat (M. Schumann et al, 2008) is an accumulation of dead organic material has been formed on the spot and has not been transported after its formation. It differs in this respect from organic sediments. A peatland is an area (with or without vegetation) with a naturally accumulated peat layer at the surface.

Peatlands contains one third of the world's soil carbon and 10% (Joosten et al, 2002) of global freshwater resources and characterized by containing more than 30% (of dry mass) dead organic matter and with a thickness not less than 30-40 cm (Frolking S. et al, 2011). A mire is a peatland where peat is currently being formed.

Peatlands could be classified into bogs and fens (M. Schumann et al, 2008) as outlined in Figure 1.

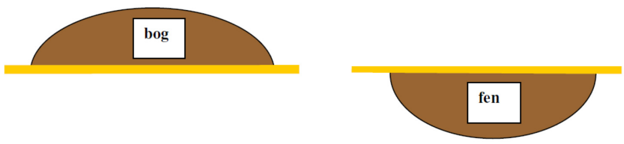

Bog	Fen
Higher than surroundings (high mires)	In landscape depressions (low mires)
Water from precipitation	Surface or ground water
Less nutrients	Rich in minerals and nutrients
Plants in fens are bigger methane producers than in bogs	

Figure 1: Fens and Bogs

1.2.2 Peatlands Distribution

Peatlands are found in (Joosten et al, 2002):

- Tropical and Sub-tropical regions: formed in very early ages (65 - 3 million years ago) is currently found as coal and lignite
- High Latitudes: Which represents the great majority of present-day peatlands originated in the last 15,000 years which are formed due to deglaciation events.

Figure 2 shows mires distribution worldwide, where we can find peatlands in Canada and Alaska, Northern Europe and Western Siberia, Southeast Asia, and parts of the Amazon basin.

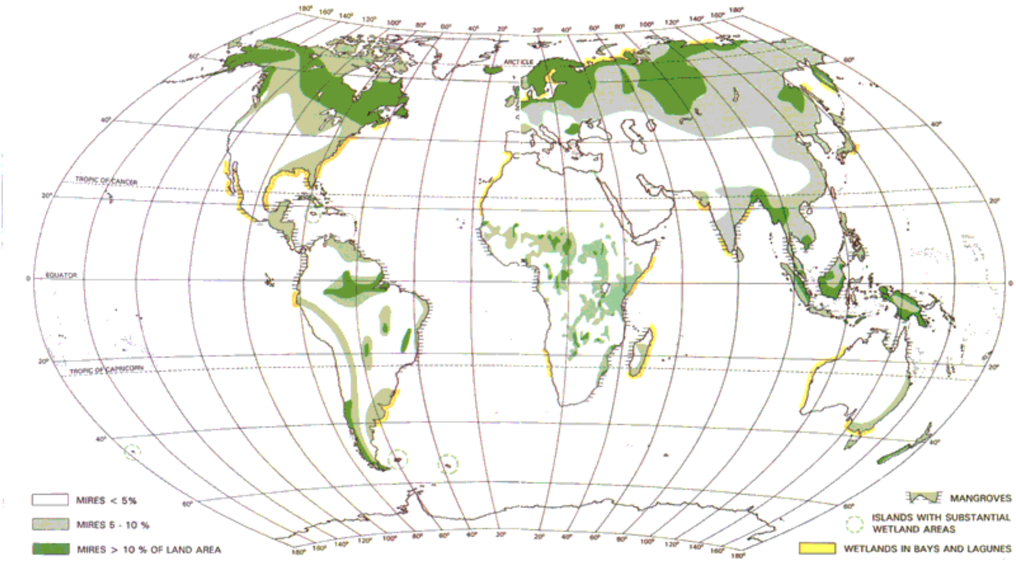

Figure 2: Distribution of Mires (Source IPS "International Peat Society")

1.3 Peatlands and Carbon Cycle

1.3.1 Photosynthesis & Respiration

Plants growth occurs by up taking CO_2 from the atmosphere during photosynthesis process (Lindsay, 2010) (Strack M. et al, 2008) and forming carbon rich material depending totally on daylight hours (Gross Primary Production – GPP). At night, in the absence of daylight, CO_2 is released as a product of the oxidation processes during respiration processes by the vegetation. This is in addition to the CO_2 released (during day and night times) resulting from the decomposition processes occurs within the aerobic zone in the acrotelm layer (Ecosystem Respiration – R_{eco}).

This could be outlined in the formulas below:

- carbon dioxide + water + light energy (by using photosynthesis) → carbohydrates + oxygen + water

- carbohydrates + oxygen → energy + carbon dioxide + water

The balance between GPP and R_{eco} is called “Net Ecosystem Exchange – NEE”. Where, Net Ecosystem Exchange (NEE) refers to GPP reduced by carbon losses by R_{eco}.

$NEE = GPP + R_{eco}$

In this study:

- GPP is presented as a CO_2 sink and has a (negative) sign
- R_{eco} is presented as a CO_2 source and has a (positive) sign
- NEE has (negative) sign indicating that peatland acts as a carbon sink
- NEE has (positive) sign indicating that peatland acts as a carbon source

1.3.2 Peatland Profile (Matrix)

Peatland profile (matrix) is commonly formed of two-layered (diplotelmic) structure (Strack M. et al, 2008), these two layers are:

	Acrotelm	**Catotelm**
Location	Upper layer of the peat	Lower and deeper layer of the peat
Organic Matter	High content and poorly decomposed	Highly decomposed
Water Table	Water table fluctuates But it is regulated by the high specific yield and the ability to shrink & swell Fluctuation occurs in the near surface zone	Permanently saturated with water
Structural Properties	• Large pore structure • High specific yield- due to large pore structure- (the ratio of the volume of water yielded by gravity drainage to the volume of soil) • Hydraulic conductivity (the rate at which water moves through the peat) is fast and generally slows with depth • Large water storage capacity due to the large pore structure	• Smaller pore structure • High total porosity • Low specific yield (less water drained by gravity) • Slower hydraulic conductivity as result of small pore sizes • Greater water retention due to the slow hydraulic conductivity

Table 1: Peatland Profile (Matrix)

The shrink & swill nature of the acrotelm could make the changes in water level not to be noticed since most of the time only the difference between ground surface and water level is measured and not the elevation itself.

1.3.3 Carbon Cycle in Peatlands

As outlined in Figure 3 below, water logging and saturation conditions reduce atmospheric oxygen diffusion into soil. The lake of oxygen makes it a limiting factor for the ecosystem respiration (illustrated above). This anaerobic conditions (Lindsay, 2010) reduce the decomposition rates to the extent such dead plant matter remains not decomposed. Over the years, such layer is covered by another layer of the dead plant matter which in turn will also remain undecomposed. Ultimately leading to accumulation of dead plant matter and consequently organic carbon is stored. This process could be called as "Peat Accumulation". Peat usually accumulates slowly, at the rate of about a one millimetre per year.

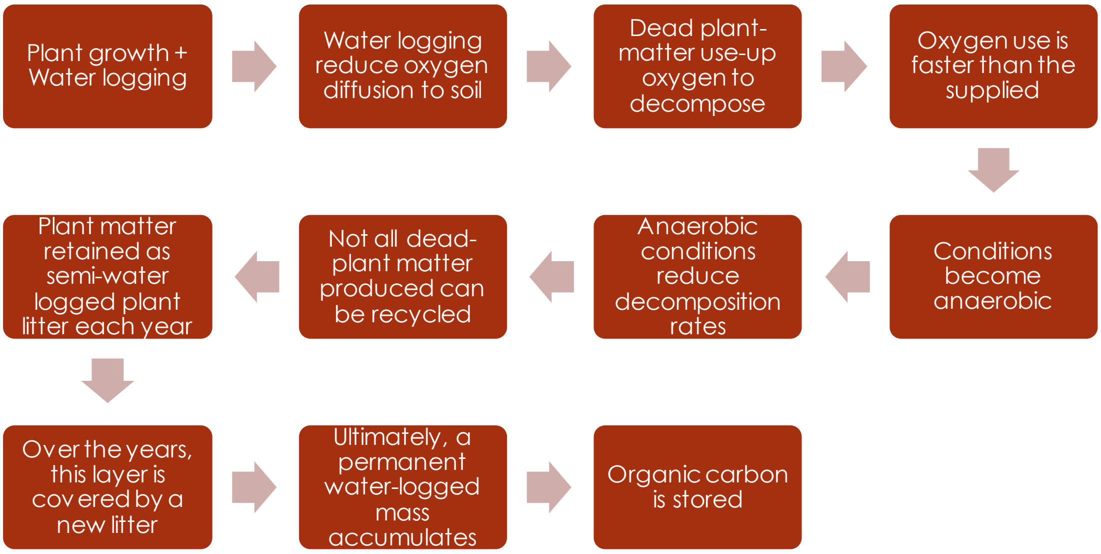

Figure 3: Processes inside Peatlands

This was also discussed by (H. Biester et al, 2014), where changes in bog hydrology leads to change in botanical composition and both causing changes in the relative abundance of *Sphagnum* and vascular plants. Which in turn affects the decomposition and peat accumulation processes. This could provide indication about the condition of the peat, since the abundance of lignin species indicate the increase of vascular plants (*Sphagnum* does not contain lignin) and increased decomposition. Accordingly, drier conditions result in change in plants abundance leading vascular plants (H. Biester et al, 2014) to become more abundant and to increase in aerobic decomposition.

1.3.4 Peatlands as a Carbon Sink

The peat accumulation process over the very long years made it as a large store of organic carbon. It is estimated that organic carbon stored in peatlands soil amounts to about 1500 Pg (Kasimir et al, 1997) (1 Pg = 10^{15} g), one-third of which is present in northern peatlands. Peatland ecosystems are globally important sources of atmospheric methane (CH_4), but at the same time they sequester carbon dioxide (CO_2) from the atmosphere. The annual carbon accumulation rates for the natural northern peatlands is estimated to be 0.1 Pg per year.

1.3.5 Peatlands Degradation

Such nature of peatlands (as a carbon sink), encouraged humans to change land use of peatlands. They used it over the years as a source of energy; additionally, the expansion in agricultural activities and the need for additional plots for planting made humans to use peatlands for such purpose. In order to be able to use peatlands, it is needed first to lower the water table by making drainage ditches to drain water outside the peatlands. Then it becomes ready for usage either for extraction in the form of blocks and used as an energy source, or adding fertilizers (as needed) and use the land for agricultural purposes. Lowering water table changes the conditions from anaerobic to aerobic conditions and enhancing the ecosystem respiration process and consequently the decomposition of dead plants. Rates of CO_2 emissions could be higher than the normal aerobic conditions due to availability of big source of organic carbon.

A study was made in Finland, Sweden & Netherlands (Kasimir et al, 1997) for GHG emissions from farmed (drained) peatlands. Table 2 shows the GHG emissions, where it could be observed that CO_2 emissions are higher in farmed peatlands even it overcome the high the Global Warming Potentials (GWP) of N_2O and CH_4.

		N_2O		**CH_4**		**Total**
	CO_2	**Actual**	**CO_2 equiv.**	**Actual**	**CO_2 equiv.**	**(CO_2 equiv.)**
Undrained peat, fen	-600	0	0	200	4900	4300
Undrained peat, bog	-900	0	0	100	2500	1600
Drained, grassland	11000 ± 4000	9 ± 5	2880	< 0.1	2	13900
Drained, cereals	20000	15 ± 11	4800	1.1	27	24800
Drained, row crop	70000	n.d.	n.d.	n.d.	n.d.	> 70000

Table 2: Emissions from organic soils (CO_2 equivalents (kg/ha/y)

1.4 Aim of this Study

As illustrated above, peatlands show a significant role in the carbon cycle and in particular the amount of carbon stored in this ecosystem. Therefore, it is important to study existing peatlands to investigate degradation indicators and peatlands contribution to GHG (weather as a sink or a source).

This work is part of the project “Carbon cycling and peat degradation of Alpine peat bogs in the Enns valley, Austria” conducted by the Working Group Geoecology, of the University of Vienna.

This Master thesis is made with the objective to find answers for the points below regarding CO_2 exchange fluxes of four different sites within the Püergschachen Moor:

- Which plant composition reveals the highest/lowest CO_2 exchange rates with respect to GPP, R_{eco} and NEE?

- How are these CO_2 release/uptake rates are affected by seasonal variabilities in terms of:
  - PAR dependency?
  - Temperature dependency?
- How do water table changes affect the CO_2 exchange rates?

As illustrated in 1.3, it is expected that GPP will be directly related to light energy (which is represented by PAR) and the exposure duration. Temperature will affect respiration, since microbial activities are increasing with temperature increase (in this study we are investigating normal and not extreme temperatures which affect the microbial community). It is also expected that water table fluctuations will affect respiration rates as a result of changing the aerobic zone depth.

1.4.1 Methodology

In order to find answers for the above questions, field measurements of CO_2 concentrations are conducted using closed chamber approach (L. Kutzbach et al, 2007) (Zerva, 2004). Then, CO_2 fluxes are calculated and used for further analysis in order to investigate the variability of GPP, R_{eco} and NEE.

The study is done between four sites presenting four (4) different plant compositions, each represented by three replicates. CO_2 fluxes are compared between each site frames and the four study sites. This will be in addition to comparing seasonal and diurnal variations of CO_2 fluxes. During data analysis soil temperature and water table variability will be also considered.

Finally, a simple model is made in order to estimate the total seasonal and annual CO_2 fluxes for each of the four study sites.

CHAPTER 2 - FIELD MEASUREMENTS

2.1 Study Area

2.1.1 Background

The Pürgschachen Moor is located (S. Glatzel et al, 2016) on the bottom of the Styrian Enns valley (Figure 4), about 1.5 km southwest of the village Ardning in the district of Liezen at an altitude of 632 m a.s.l. It is a pine peat bog with an area about 62 ha (620,000 m^2). The valley bogs were formed as a result of formation of postglacial lakes on impermeable loamy clay.

Figure 4: Püergschachen Moor (source: www.moor.ardning.at)

This intact valley peat bog with a closed peat moss cover presents a good example of the formerly widely distributed peatlands of inner-alpine valleys. Due to the importance of the study area, since 1991, the peat bog is part of the international and intergovernmental treaty of the Ramsar Convention, constituting a convention on wetlands for the conservation and wise use of wetlands and their resources. The study area is considered a part of the network of nature protection areas Natura 2000 and is protected as European nature reserve.

2.1.2 Sites and Frames

For the purpose of this study, four sites were selected inside the study area to present four different plant compositions (Table 3 and Figure 5). Three replicates are used to present each site by fixing three frames for field measurements.

Site	Dominating plant species	
PM1	*Eriophorum vaginatum & Rhynchospora alba*	Figure 6
PM2	*Pinus mugo* < 35 cm	Figure 7
PM3	*Calluna vulgaris*	Figure 8
PM4	*Pinus mugo* (35-60 cm)	Figure 9

Additionally, all four sites are covered with *Sphagnum* species

Table 3: Plant Species in Study Sites

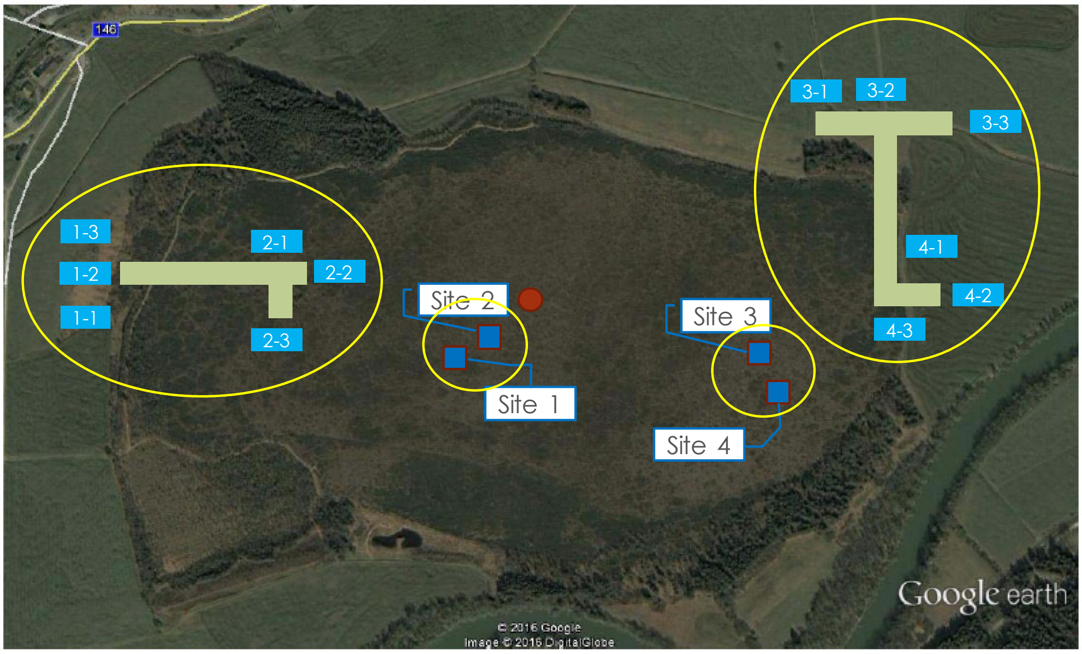

Figure 5: Sites and Frames Distribution in Study Area

Site PM1-1

Site PM1-2

Site PM1-3

Figure 6: The three Frames in Site PM1

Site PM2-1

Site PM2-2

Site PM2-3

Figure 7: The three Frames in Site PM2

Site PM3-1 Site PM3-2 Site PM3-3

Figure 8: The three Frames in Site PM3

Site PM4-1 Site PM4-2 Site PM4-3

Figure 9: The three Frames in Site PM4

2.2 CO_2 Measurement Approaches

CO_2 exchange could be measured (L. Kutzbach et al, 2007) by using different approaches such as eddy covariance approach or closed chamber approach.

2.2.1 Eddy Covariance Approach

Fluxes are measured by using atmospheric measurements within the atmosphere boundary layer. Where, air flow during the horizontal flow takes the form of rotating vortices (rotating eddies) and the measurement tower is measuring the vertical movement of the components of these eddies (such as GHG). Basically, it measures the concentrations in consecutive eddies and calculate the fluxes based on the time interval between each measurement.

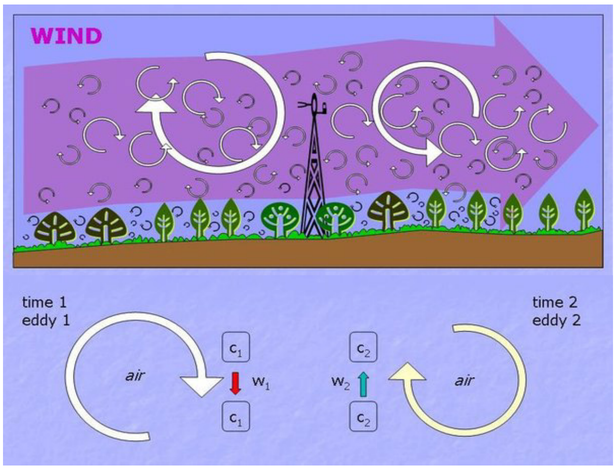

Figure 10: Eddy Covariance Principals

As illustrated in Figure 10 (G. Burba et al, 2010), at time 1 we have eddy 1 in which air parcel c1 moves downward with speed w1. Also, at time 2 we have eddy 2 and air parcel c2 with speed w2. From these factors and knowing how many molecules of the concerned water vapour (or any other gas), vertical fluxes can be calculated.

Which could be presented by the basic formula (M. Litvak, 2007) illustrated below:

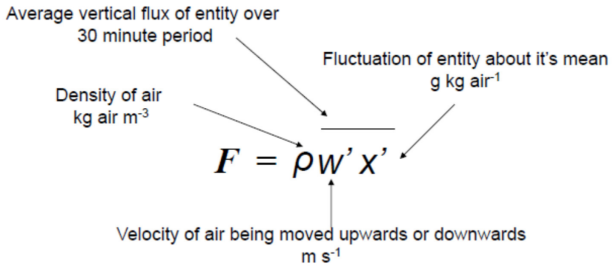

Figure 11 shows the eddy tower used in the study area.

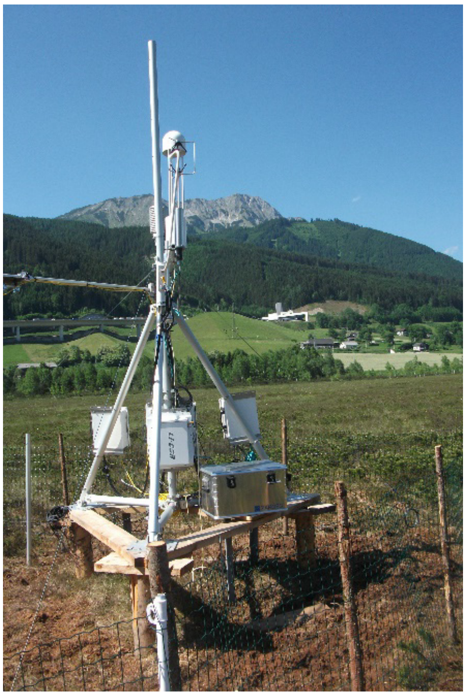

Figure 11: Eddy Tower in Study Area

This approach results in enormous continuous measurements which provide high temporal resolution but on the same time cannot provide measurements for specific locations within the study area.

2.2.2 Closed Chamber Approach

As outlined in Figure 12, closed chamber is basically composed of a frame fitted to the soil and a chamber to be fitted on top of the frame (with proper sealing to prevent gas penetration either in- or out-side the chamber). Then gas is collected and gas concertation is measured.

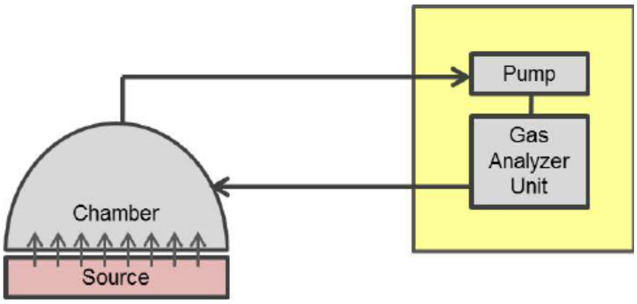

Figure 12: Closed Dynamic Chamber - Schematic Diagram (source: Sutitarnnontr et al., 2012)

This approach as per (Zerva, 2004) is used back more than 80 years for gas measurements and could be classified under two most widely used techniques as outlined in Table 4.

	Dynamic Closed Chamber	Static Closed Chamber
Air circulation	Air is circulated from the chamber to gas analyser (Infra-Red Gas Analyser IRGA) and then returned back to the chamber	Air is not circulated and a certain volume of atmosphere is sealed above the soil surface
Measurement Duration	Measurements are taken instantly by the IRGA and the chamber is placed between 2-3 minutes	The chamber is placed for a longer duration (between 20-60 minutes) to allow gas accumulation
Gas Sampling	Gas is measured by the IRGA and no samples are taken	Gas samples are taken and then gas is analysed by gas chromatographic or infrared analysis.

Table 4: Comparison between Dynamic and Static Closed Chamber Approach

During chamber measurements, some effects occur and need to be taken into consideration, including (Zerva, 2004) (L. Kutzbach et al, 2007):

- Soil disturbance: Due to chamber placement into the soil and release CO_2 from the soil pores. This could be overcome by leaving the chambers in place for some time before measurement takes place.
- Temperature & moisture changes: Closure of the chamber produces alterations in soil temperature and moisture in the chamber, which consequently will cause changes in the CO_2 efflux. This effect is more considerable in the static approach

due to the long measurement period, and very small in the dynamic approach as a result of the short period.

- Concentration gradient changes: Also, this is due to closure of the chamber leading to increase in CO_2 concentration inside the chamber resulting in decreasing the concentration gradient through soil profile. Again, the period of chamber placement plays a role and this effect is very small in the dynamic approach.
- The closed static chamber method has sometimes been criticised for underestimating the soil CO_2 efflux at low flux rates and severely underestimating it at high flux rates, compared to the closed dynamic chamber method which has been shown to be more accurate for a wide range of flux rates
- The closed static chamber method is currently the most common method for the measurement of other trace gases such as nitrous oxide (N_2O) and methane (CH_4).

2.2.3 Approach Used

As the purpose of this study is to investigate CO_2 fluxes for different sites within the study area, the eddy covariance will not be used and the closed chamber approach will be used.

Considering the discussion above and the comparison between dynamic and static closed chambers (Item 2.2.2), the dynamic chamber was the selected measurement approach.

2.3 Instruments and Tools Used

2.3.1 Chamber Frames

Frames (Bogdan H. Chojnicki et al, 2009) were fixed at the selected different sites these frames served the below objectives:

- Maintain measurements consistency over the study duration at the same specific site
- Prevent gas leakage
- Maintain chamber stability during measurement

Figure 13: Frame fitted in the Site

The frame was made from aluminium square collar (75 x 75 x 20 cm) and was inserted about 17 cm into the substrate. Figure 13 shows one of the frames used at the study area.

2.3.2 Closed Dynamic Chambers

Following (Bogdan H. Chojnicki et al, 2009) and (S. Beetz et al, 2013), two types of closed dynamic chambers were used both of them was of size (78 × 78 × 53.5 cm) except for PM4-3 the chamber height was (103.5 cm) to provide enough overhead space due to plant composition height:

- Transparent Chamber (Figure 14): Was made of Plexiglas (3 mm thick) and used to measure the Net Ecosystem Exchange (NEE). The chamber material reduced Photosynthetic Active Radiation (PAR) up to 5% (Bogdan H. Chojnicki et al, 2009)
- Opaque Chamber (Figure 15): Was made of white PVC (3 mm thick) in order to reduce sun radiation influence and measure ecosystem (autotrophic and heterotrophic) respiration (R_{eco})

Figure 14: Transparent Closed Dynamic Chamber

Figure 15: Opaque Closed Dynamic Chamber

Each chamber was equipped with two fans (Bogdan H. Chojnicki et al, 2009) for air circulation inside the chamber. The tightness of chambers during the measurement was assured by a rubber gasket installed around of the chamber's lower edge.

2.3.3 Infra-Red Gas Analyser (IRGA)

Gas concentration is measured by determining the absorption of an emitted infrared light through the air sample (i.e. measuring how much of the air is absorbed by the air). Figure 16 shows that each GHG has its specific absorption characteristics which help to measure the desired gas only. By comparing the determined the absorbed infrared with a reference measurement the gas concentration could be determined.

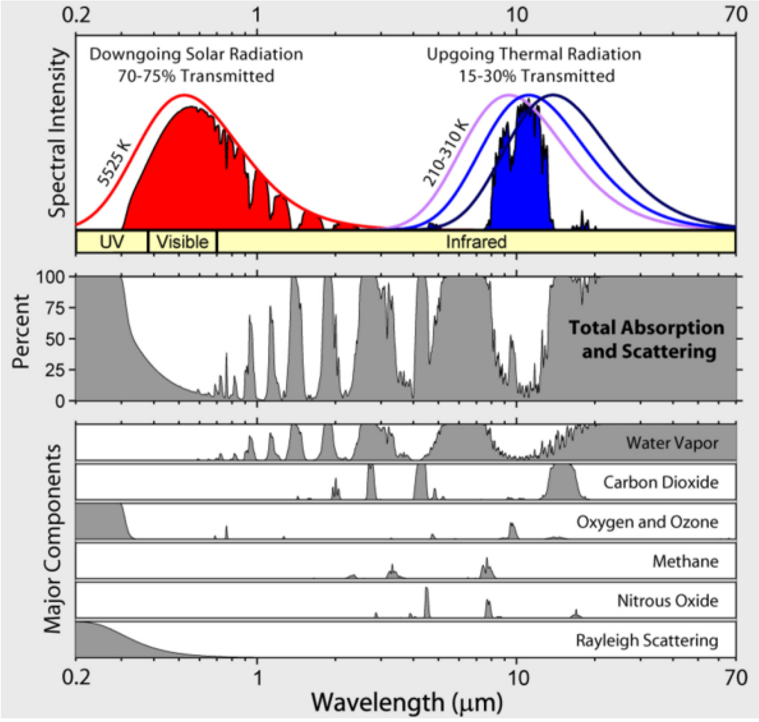

Figure 16: Radiation Adsorption by GHG (source: clivebest.com)

The suction pump allows the gas inside the closed chamber to pass through the IRDA in order to measure CO_2 concentrations in (ppm). In this study a Gas Emission Research Detector (GERD) LI-820 "CO_2 Gas Analyser" (Figure 17) manufactured by *LI-COR®* is used.

Figure 17: LI-820 "CO_2 Gas Analyser"

This instrument allows for many concentration measurements to be taken during measurement period and allows also, as will be explained below, the calculation of gas fluxes.

2.4 Measured Data

2.4.1 Measurement Plan

Measurement campaigns were conducted with the aim to obtain representing CO_2 fluxes of the four seasons (spring, summer, autumn & winter) as well as over the day hours. Also, attention was made to conduct measurement sessions covering the four sites by taking measurements at the replicate frames within each site. Each measurement lapsed 120 and 180 seconds for the transparent and opaque chambers respectively.

Weather had a limiting factor during measurements specially during winter, early spring and late autumn. Also, the need of day light to conduct the measurements affected the window of availability to conduct the measurements. Specially, time was needed to move and mobilize the instruments & tools between the four sites.

The author of this thesis participated only in the field measurements during June 2015 and July 2015 for the purpose of this study as well as during May 2016 for extended measurements (each was 2-3 days).

Since all measurement campaigns were conducted from April to October (except for a very few measurements were done in February), all time mentioned in this thesis are based on CEST.

2.4.2 GERD Measurements

CO_2 concentration were measured by GERD (as explained above in 2.3.3). The output measured data covered the following points:

- Date, Time and Record Number
- Site and Session number
- CO_2 concentration (ppm)
- PAR (Photosynthetic active radiation (µmol photon^{-1} m^{-2} s^{-1})
- Temperature (in Chamber – Air – Soil at: 2, 5 & 10 cm depth)
- Chamber area and height
- Opaque (D) or Transparent (T) Chamber
- Pump pressure & temperature – Battery voltage

Figure 18 shows sample of the GERD output data file.

```
Datum;Zeit;SessionNr;RecordNr;Standort;CO2 ;PRE ;LI820-Temp;PAR ;TH ;TL ;TB2 ;TB5 ;TB10 ;Bat-Volt;HF;HH;HK;HA;
2015/08/10;06:20:48;204722848;1;PM01-1;668.88;92.24;50.89;9.64;9.27;8.32;15.38796;17.38669;19.71357;11.88;0.6084;0.535;3;T;
2015/08/10;06:20:48;204722848;2;PM01-1;668.88;92.24;50.89;9.64;9.27;8.32;15.38796;17.38669;19.71357;11.88;0.6084;0.535;3;T;
2015/08/10;06:20:49;204722848;3;PM01-1;669.69;92.24;50.89;7.84;9.24;8.32;15.38796;17.38669;19.7434;11.84;0.6084;0.535;3;T;
2015/08/10;06:20:50;204722848;4;PM01-1;669.32;92.24;50.89;3.33;9.21;8.32;15.4178;17.44636;19.7434;11.84;0.6084;0.535;3;T;
2015/08/10;06:20:52;204722848;5;PM01-1;669.52;92.25;50.89;8.74;9.21;8.32;15.4178;17.41652;19.7434;11.85;0.6084;0.535;3;T;
2015/08/10;06:20:53;204722848;6;PM01-1;669.11;92.25;50.89;8.74;9.18;8.35;15.4178;17.41652;19.7434;11.88;0.6084;0.535;3;T;
2015/08/10;06:20:54;204722848;7;PM01-1;668.78;92.25;50.91;10.54;9.21;8.32;15.44763;17.38669;19.7434;11.88;0.6084;0.535;3;T;
2015/08/10;06:20:56;204722848;8;PM01-1;669.41;92.25;50.91;10.54;9.21;8.32;15.4178;17.41652;19.71357;11.88;0.6084;0.535;3;T;
2015/08/10;06:20:57;204722848;9;PM01-1;670.06;92.25;50.91;9.64;9.15;8.32;15.4178;17.44636;19.71357;11.84;0.6084;0.535;3;T;
2015/08/10;06:20:58;204722848;10;PM01-1;671.50;92.25;50.91;10.54;9.15;8.32;15.4178;17.38669;19.7434;11.84;0.6084;0.535;3;T;
2015/08/10;06:21:00;204722848;11;PM01-1;671.37;92.25;50.91;9.64;9.15;8.29;15.4178;17.41652;19.7434;11.86;0.6084;0.535;3;T;
2015/08/10;06:21:01;204722848;12;PM01-1;670.22;92.24;50.91;10.54;9.12;8.32;15.4178;17.44636;19.71357;11.88;0.6084;0.535;3;T;
2015/08/10;06:21:02;204722848;13;PM01-1;670.74;92.24;50.91;9.64;9.09;8.32;15.38796;17.41652;19.77323;11.88;0.6084;0.535;3;T;
```

Figure 18: Sample of GERD output data

As explained by (Bogdan H. Chojnicki et al, 2009), we could observe from Figure 19 the reduction of CO_2 concentration during the measurement session of the transparent chamber. As illustrated in 1.3.1, during daylight the plants performs the GPP process using the solar radiation as a source of energy (which is represented by the PAR). During this process, CO_2 is consumed and consequently the concentration is getting lower with time. Additionally, ecosystem respiration process still on going and the resulting curve is the balance between GPP and R_{eco} representing the ecosystem NEE. When the concentration goes down this mean that the site is not a carbon source (i.e. a carbon sink). Accordingly, in case of transparent chamber, the measured CO_2 concentration represent the NEE for this ecosystem.

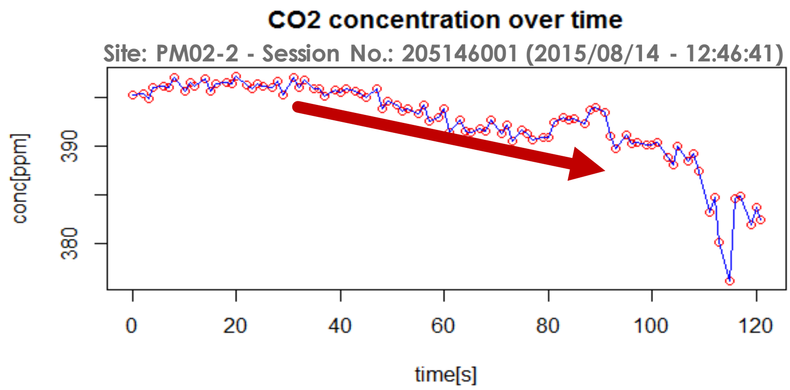

Figure 19: Sample Measurement - Transparent Chamber measurement session

While as illustrated in Figure 20, CO_2 concentration increases during the opaque chamber measurements as a result of the ecosystem respiration process only (R_{eco}). Since no GPP process due to the absence of light.

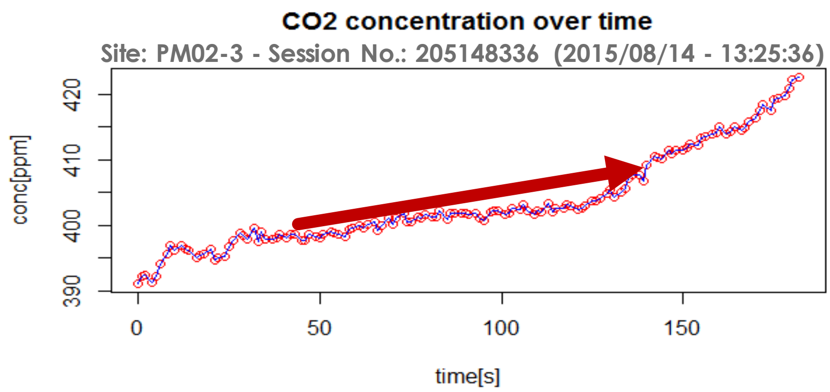

Figure 20: Sample Measurement - Opaque Chamber measurement session

2.5 CO_2 Flux Calculations

2.5.1 Methodology

Flux is the flow rate of a property per unit area, which in this study case will be the flow rate of CO_2 per unit area. This could be simplified as the area below the curve (e.g. as in Figure 19 and Figure 20), which will indicate the total quantity of CO_2, divided by measurement duration and chamber area (mass per time per area).

Using the closed dynamic chamber approach for field data measurement in this study (as explained in 2.3) resulted in an enormous amount of measured data. Which lead to the need for an automated mechanism for flux calculations. Accordingly, Package 'flux' (Version 0.3-0 - Date 2014-04-23) prepared by (Jurasinski et al, 2014) was used.

This automated package enables the performance of several iterations in order to obtain the best fitting for the regression line for the gas concentrating curve which in turn provide more accurate results than manual calculation. Additionally, this package saved a considerable time in calculating CO_2 fluxes for the various field measurements.

For the purpose of using this package a R-script (Annex 1 – CO2 Fluxes Calculations' *R-Script*) was made to convert the output data recorded by the GERD into input data files readable by the package.

2.5.2 Calculated CO_2 Fluxes

Table 5 shows sample of the calculated CO_2 fluxes (g m^{-2} h^{-1}) for some of the field measurement sessions.

Site	Date	Time	SessionNr	CO2.unit	CO2.flux	Transp_Opaque	PAR	Air_Temp
PM02-1	8/10/2015	7:16:44	204726204	g	0.572	TRUE	228.952	13.115
PM02-1	8/10/2015	7:57:08	204728628	g	0.933	D	391.980	15.242
PM03-1	8/10/2015	11:21:05	204740865	g	-0.959	TRUE	1466.336	29.775
PM03-1	8/10/2015	11:57:17	204743037	g	0.578	D	1545.602	31.442
PM04-1	8/13/2015	6:25:41	205023141	g	0.740	TRUE	14.317	9.121
PM04-1	8/13/2015	7:14:18	205026058	g	0.978	D	208.301	12.413
PM03-1	8/13/2015	7:38:48	205027528	g	-0.363	TRUE	331.749	15.364
PM03-1	8/13/2015	8:13:08	205029588	g	0.662	D	528.499	18.890
PM04-3	8/14/2015	11:23:22	205141002	g	-0.322	TRUE	1410.062	29.186
PM04-3	8/14/2015	11:36:04	205141764	g	0.859	D	1462.983	28.747
PM01-1	8/14/2015	12:02:48	205143368	g	-1.060	TRUE	1494.842	30.481
PM01-1	8/14/2015	12:29:07	205144947	g	0.875	D	1563.089	29.591

Table 5: Sample CO_2 Calculated Fluxes

Calculated fluxes (Table 5) were compared with CO_2 fluxes presented in other literatures (Table 6) for the purpose of verification the order of magnitude of the calculated fluxes under this study. From this comparison, it could be noted that the calculated fluxes under this study are in the same order of magnitude with the fluxes.

Literature / Subject	CO_2 Flux		
	Amount	Units	g m^{-2} h^{-1}
Net ecosystem CO2 exchange in a boreal peatland, northern Manitoba Bellisario, L M et. al. (1998)			
NEP	-2	g CO_2-C m^{-2} d^{-1}	-0.306
	4		0.612
Measurements of Carbon Dioxide Fluxes by Chamber Method at the Rzecin Wetland Ecosystem, Poland Bogdan H. Chojnicki et. al. (2010)			
R_{eco}	2.65	µmol CO_2 m^{-2} s^{-1}	0.420
	14.76		2.338
NEE	0.06		0.010
	-11.82		-1.872
CO2 exchange of a temperate fen during the conversionfrom moderately rewetting to flooding Franziska Koebsch et. al. (2013)			
R_{eco}	1090	g CO_2-C m^{-2} a^{-1}	0.456
	1639		0.686
Net CO_2 (2009 - 2010 - 2011)	-333.3	g CO_2-C m^{-2} $0.5a^{-1}$	-0.279
	-294.1		-0.246
	-352.4		-0.295
Winter emissions of carbon dioxide, methane and nitrous oxide from a minerotrophic fen under nature conservation management in north-east Germany - V. Huth et. al. (2012)			
CO_2 effluxes	-160	mg m^{-2} h^{-1}	-0.160
	650		0.650

Table 6: CO_2 Fluxes in other Literatures

CHAPTER 3 - RESULTS

3.1 Data Grouping

As explained in 2.4.1, measurement sessions were spread over the year with a total of 1416 measurement sessions. Some of the calculated fluxes was eliminated from the study as explained below:

- Fluxes with unrealistic values: Having negative flux in opaque chamber measurement session, which could not happen. As explained in 1.3.1 respiration processes are represented by positive sign and in 2.3.2 opaque chambers are used to measure respiration processes. This could be due to error in defining the measurement session at field.
- Due to the field measurements limitations (as outlined in 2.4.1), a very limited number of measurements were taken during winter measurements campaign (on 11^{th} & 12^{th} February 2016), only two transparent measurements at 11:00 and one transparent measurement at 17:00 were taken in Site PM1 – Frame 1. Also, the low PAR values during these measurements (51.4 μmol photon^{-1} m^{-2} s^{-1}) resulted in no flux calculations. Therefore, winter season could not be represented.
- Some of the calculated opaque fluxes with zero value showing no respiration activities, which could be resulted from some measurements errors
- One unrealistic flux (-16.0874 g m^{-2} h^{-1}) in transparent measurements

The total of the eliminated fluxes was 25 with a percentage of 2% of the total number of calculated fluxes.

Table 7, shows the distribution of the calculated fluxes over the study sites. Table 8 and Table 9 show the seasonal distribution.

Site	Transparent	Opaque	Sum
PM1	302	85	**387**
PM2	277	79	**356**
PM3	282	60	**342**
PM4	242	61	**303**
Sum	**1103**	**285**	**1388**

Table 7: Distribution of Calculated Fluxes over Study Sites

Season	PM1	PM2	PM3	PM4	Sum
Spring	51	36	54	40	**181**
Summer	207	211	161	161	**740**
Autumn	44	30	67	41	**182**
Sum	**302**	**277**	**282**	**242**	**1103**

Table 8: Seasonal Distribution of Calculated Fluxes - Transparent Chamber

Season	PM1	PM2	PM3	PM4	Sum
Spring	16	7	6	6	**35**
Summer	61	61	46	49	**217**
Autumn	8	11	8	6	**33**
Sum	**85**	**79**	**60**	**61**	**285**

Table 9: Seasonal Distribution of Calculated Fluxes - Opaque Chamber

3.2 Seasonal Variability

The variability of CO_2 fluxes between spring, summer and autumn with respect the four sites were investigated in order to provide an overview about the overall behaviour of the study area.

3.2.1 CO_2 Fluxes Distribution with Respect to PAR

There is low correlation between NEE and PAR in spring (r=-0.36) and in autumn (r=-0.38); but a high correlation was shown in summer (r=-0.56) as illustrated in Figure 21. From Table 10, we could observe, at the same PAR category, summer shows higher NEE fluxes than in spring and autumn which suggests that NEE fluxes are affected by other factors in addition to PAR. Even with the low correlation in spring and autumn, by comparing NEE fluxes at the same PAR category, it could be noticed that spring is higher than in autumn.

	Average NEE (g m^{-2} h^{-1})		
PAR Category	**Spring**	**Summer**	**Autumn**
< 100	0.080	0.511	0.234
100 - 350	-0.264	-0.130	-0.049
350 - 700	-0.664	-0.500	0.081
700 - 1150	-0.337	-0.599	-0.180
1150 - 1500	-0.531	-0.754	-
1500 <	-0.388	-0.573	-

Table 10: Seasonal average NEE per PAR categories

From the distribution of NEE with respect to PAR, schematic trend line could be made as illustrated in Figure 21. It could be observed from such trend that, NEE have positive values at low PAR (< 100 µmol photon^{-1} m^{-2} s^{-1}) indicating release of carbon suggesting that production (GPP) is less than respiration (R_{eco}). With PAR increase, NEE tends to be negative indicating carbon uptake and which increases with PAR increase, indicating increase in the production process (GPP). However, with more increase in PAR (than 1150-1500 µmol photon^{-1} m^{-2} s^{-1}) production rate starts to be lower again.

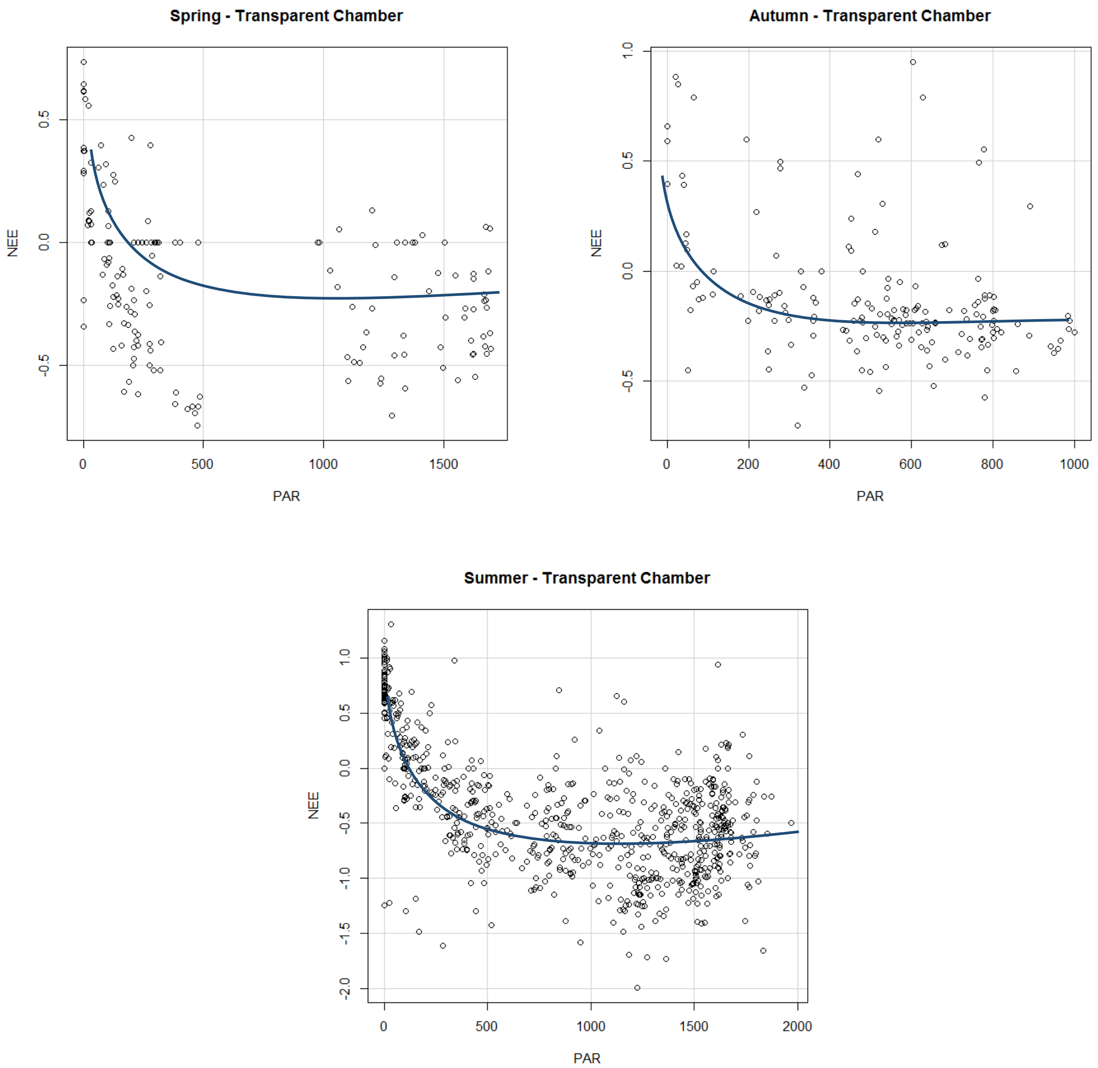

Figure 21: Distribution of NEE (g m^{-2} h^{-1}) with respect to PAR (µmol $photon^{-1}$ m^{-2} s^{-1})

3.2.2 CO_2 Fluxes Distribution with Respect to Soil Temperature

Soil temperature at 2cm, 5cm and 10cm depths were measured during measurement sessions, Figure 22 and Figure 23 show the distribution of CO_2 fluxes with respect to soil temperature at 2cm. There is low correlation between NEE and soil temperature for the total year measurements (r= -0.236), this low correlation is also noticed in the study seasons spring, summer and autumn (r= 0.148, -0.187 & -0.005 respectively).

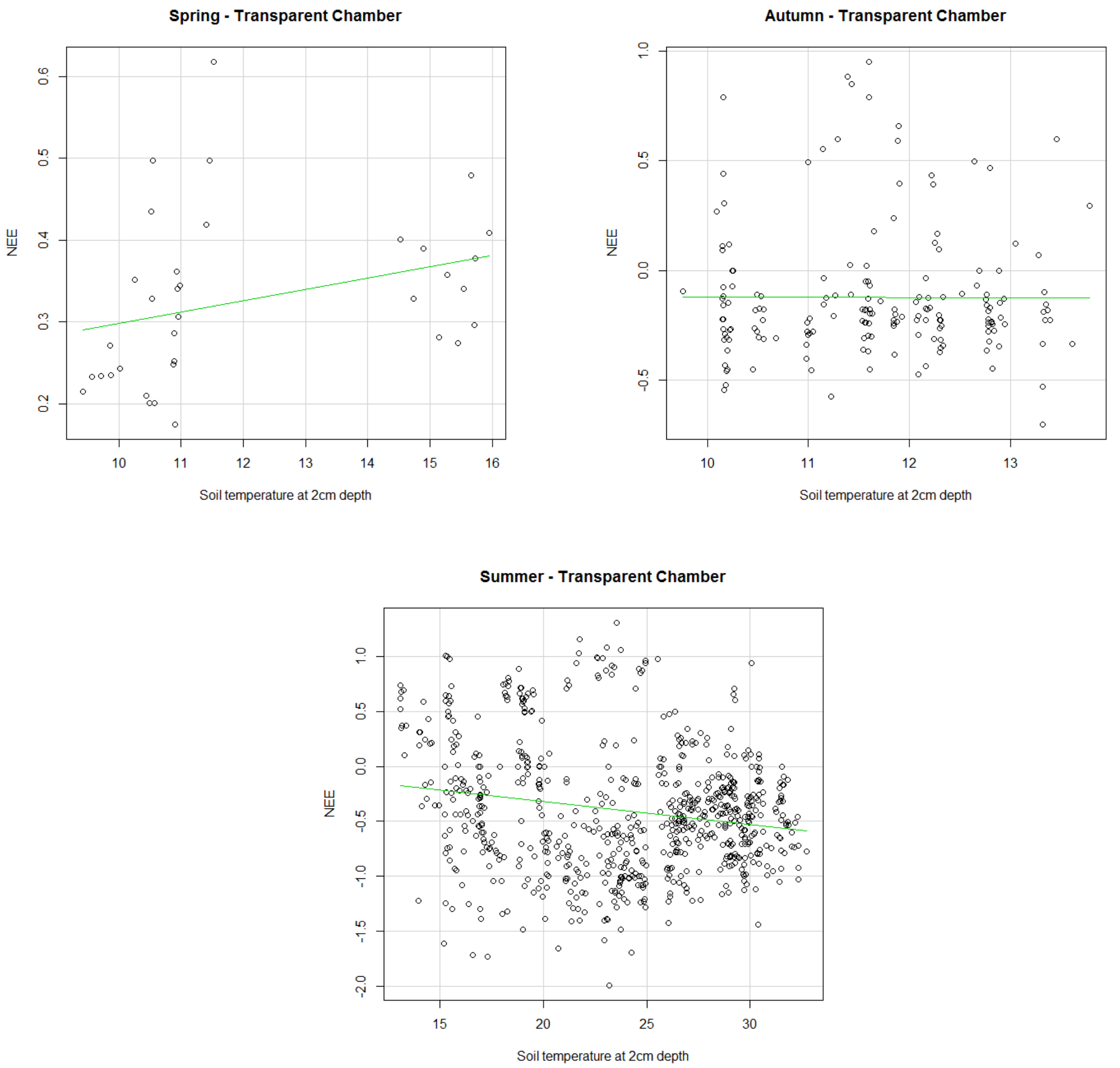

Figure 22: Distribution of CO_2 Fluxes (g m^{-2} h^{-1}) with respect to Soil Temperature (℃) at 2cm Depth – Transparent Chamber

On the other hand, high correlation was observed between respiration (R_{eco}) and soil temperature (r= 0.763). Summer showed the highest correlation (r=0.445), then spring (r=0.318) and a very low correlation in autumn (r=0.084). Summer measurements showed higher respiration than spring and autumn, which is similar to (Bogdan H. Chojnicki et al, 2009) discussion, where in summer the temperature is the highest and aboveground biomass reach the maximum stage development.

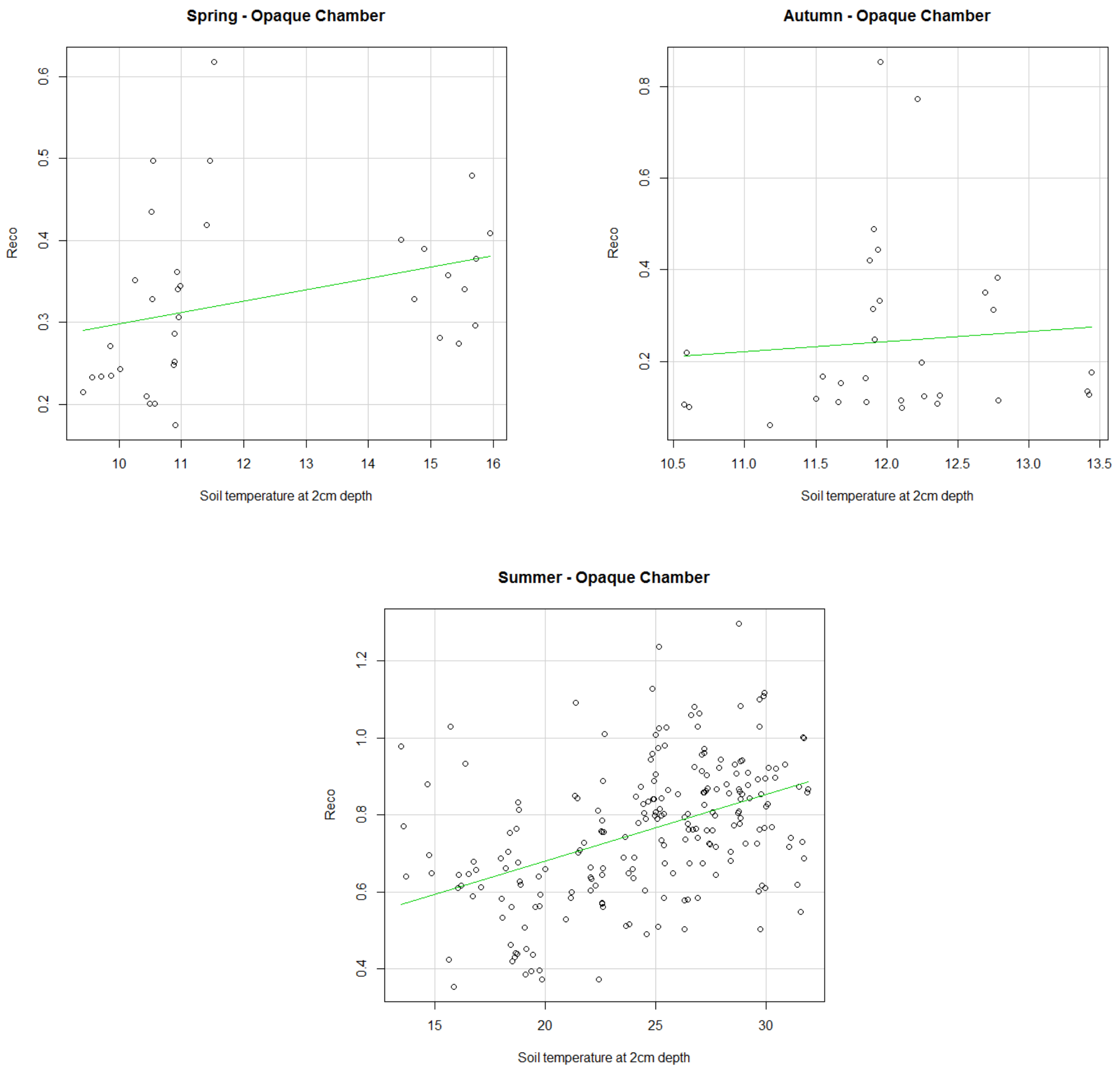

Figure 23: Distribution of CO_2 Fluxes (g m^{-2} h^{-1}) with respect to Soil Temperature (℃) at 2cm Depth – Opaque Chamber

3.2.3 CO_2 Fluxes Distribution with Respect to Day Time

Average summer measurements, as presented in Figure 25 and Table 11, show carbon release at early morning measurement (at 6:00), then afterwards the system starts to uptake carbon with increasing fluxes up to certain time (the average values corresponds to 10:00) and the uptake starts to be lower until carbon release starts again in late afternoon (at 18:00 and upwards). This NEE behaviour follows the same behaviour of GPP along day hours; suggesting that, during day hours, the net carbon uptake/release of the system is controlled by the production process.

The occurrence of carbon release in the early morning and late afternoon, which corresponds to the low PAR values, is related to the low production process by plants either at the start of day hours or at end of the day hours.

Day Hours	R_{eco} (g m^{-2} h^{-1})			NEE (g m^{-2} h^{-1})			GPP (g m^{-2} h^{-1})		
	Spring	Summer	Autumn	Spring	Summer	Autumn	Spring	Summer	Autumn
6:00		0.613			0.278			-0.335	
7:00		0.729			-0.292			-1.021	
8:00	0.298	0.609		-0.064	-0.569		-0.362	-1.178	
9:00	0.353	0.651		-0.480	-0.782		-0.833	-1.433	
10:00	0.508	0.732		-0.621	-0.994		-1.129	-1.726	
11:00	0.237	0.775	0.122	-0.551	-0.704	-0.188	-0.788	-1.479	-0.310
12:00	0.239	0.834	0.141	-0.335	-0.568	-0.135	-0.574	-1.402	-0.276
13:00	0.236	0.791	0.098	-0.374	-0.641	-0.167	-0.610	-1.432	-0.265
14:00	0.232	0.824	0.114	-0.503	-0.596	-0.205	-0.735	-1.420	-0.319
15:00	0.210	0.779	0.254	-0.338	-0.507	-0.055	-0.548	-1.286	-0.309
16:00		0.795	0.293		-0.316	-0.293		-1.111	-0.586
17:00		0.679	0.146		-0.253	0.039		-0.932	-0.107
18:00	0.338	0.795		-0.091	0.103		-0.429	-0.692	
19:00	0.381	0.699		-0.014	0.380		-0.395	-0.319	
20:00		0.816			0.858			0.042	
21:00		0.880			0.741			-0.139	

Table 11: Day time average hourly values of seasonal R_{eco}, NEE and GPP hourly

The pattern of GPP over the day hours matches the PAR pattern, which confirms the correlation with PAR as discussed in 3.2.1 (above); increasing PAR increases GPP up to a limit which is related to the photosynthesis light response (PAR ≅ 1000 µmol photon^{-1} m^{-2} s^{-1}) as shown in Figure 24 and Table 12. From Figure 24, PAR starts to reduce with day time and consequently GPP becoming lower as shown in Figure 25.

Temperature also affects the system NEE, by comparing Figure 25 and Figure 24 we could observe that system uptake increases with increasing temperature and getting lower with reducing temperature. However, as discussed in 3.2.2, the temperature effect has low correlation with the NEE.

Day Hours	Soil Temp. at 2cm (°C)			PAR (µmol photon^{-1} m^{-2} s^{-1})		
	Spring	Summer	Autumn	Spring	Summer	Autumn
6:00		14.77			56.76	
7:00		15.82	11.41		311.06	23.31
8:00	10.85	18.76	11.60	27.79	472.08	60.65
9:00	12.85	19.73	10.43	835.25	932.12	203.65
10:00	15.65	23.43	12.08	1079.73	1242.87	359.28
11:00	9.95	25.69	11.90	345.87	1423.72	605.03
12:00	15.52	26.36	11.23	985.20	1378.03	843.01

Day Hours	Soil Temp. at 2cm (°C)			PAR (µmol photon^{-1} m^{-2} s^{-1})		
	Spring	Summer	Autumn	Spring	Summer	Autumn
13:00	18.31	26.86	11.64	904.45	1602.56	743.75
14:00	18.11	27.47	12.35	1011.07	1287.00	521.35
15:00	17.02	26.74	11.36	371.68	1227.82	539.87
16:00		27.14	11.44		898.32	398.85
17:00		26.21	12.80		564.08	109.67
18:00	19.42	23.67	11.91	294.92	277.75	0.57
19:00	18.39	23.31		85.21	88.49	
20:00	15.31	21.98		1.04	1.64	
21:00		21.85			1.00	

Table 12: Day time average hourly values of seasonal temperature and PAR

Similar behaviour could be observed in spring and autumn but will less values as shown in Table 11, indicating that temperature also affects the GPP process since summer shows higher recorded temperature than spring and autumn.

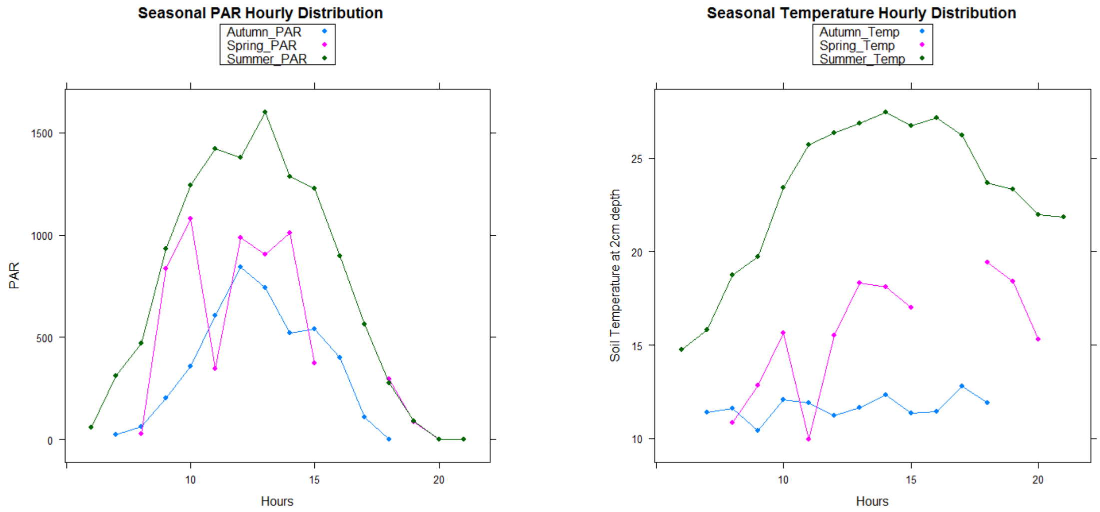

Figure 24: Day time average hourly distribution of seasonal PAR (µmol photon^{-1} m^{-2} s^{-1}) and temperature (℃)

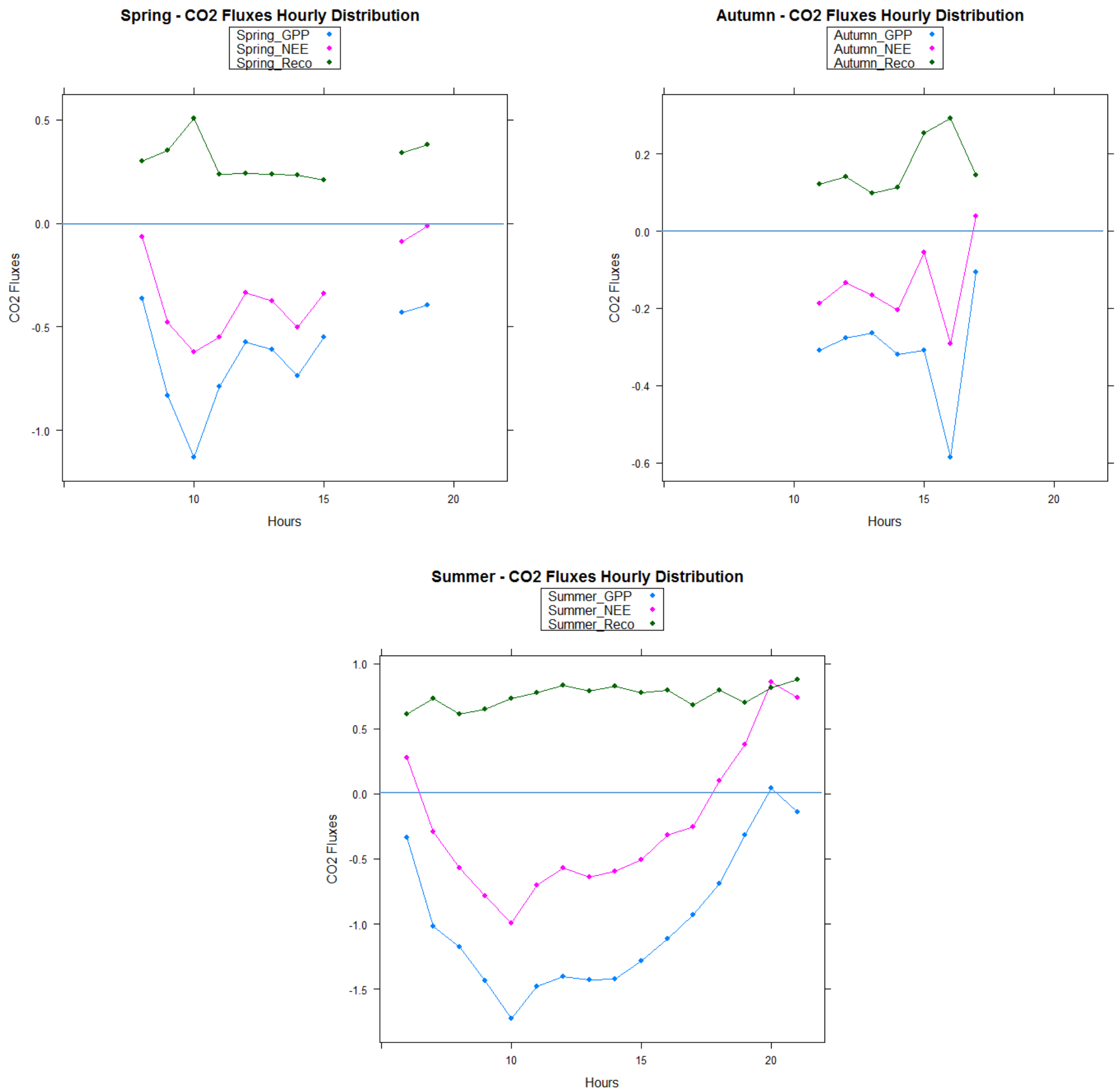

Figure 25: Day time average hourly distribution of seasonal CO_2 fluxes (g m^{-2} h^{-1})

3.2.4 Seasonal Variability Summary

Ecosystem Respiration (R_{eco}):

The discussion under this item 3.2 shows that respiration (R_{eco}) is affected by temperature changes over the day time as well as between spring, summer and autumn. Table 11 shows that at the same time, respiration in summer has higher values than spring then autumn. Comparing this with Table 12, it could be noticed that at the same time temperature in summer is higher than spring then autumn. This respiration/temperature relationship is not only related to seasonal variability but also to temperature changes over the day time hours. All of this resulting in high correlation between respiration and soil temperature (r= 0.763) as shown in 3.2.2.

Gross Primary Production (GPP):

Table 11 shows that GPP increases with increasing PAR as discussed under 3.2.1 showing the change in NEE with PAR increase up to a limit (PAR=1150-1500 µmol photon^{-1} m^{-2} s^{-1} production) which is related to photosynthesis light response curve then GPP rate starts to be lower. Comparing same PAR in Table 12 between the three seasons shows that summer present higher GPP (from Table 11) than spring, suggesting that PAR is not only the factor affecting GPP but it is also affected by seasonal climatic variability.

As an example: PAR ≅ 900 (µmol photon^{-1} m^{-2} s^{-1}) occurs in summer at 9:00 and spring at 13:00 with corresponding soil temperature of 19.73°C and 18.31°C respectively. The related GPP for summer was -1.433 g m^{-2} h^{-1} and spring -0.610 g m^{-2} h^{-1}.

Net Ecosystem Exchange (NEE):

This behaviour of R_{eco} and GPP during daytime lead that NEE shows CO_2 release at the lowest PAR categories (as discussed in 3.2.1) as a result of the low production and with increasing production CO_2 uptake increases and then starts to be lower with GPP reduction (as illustrated in 3.2.3), with higher fluxes in summer than spring then autumn.

3.3 Comparison between the Four Sites

3.3.1 PAR Categorization

To investigate further the effect of PAR on the resulting CO_2 fluxes and consequently the NEE of the ecosystem in four study sites, PAR values were categorized into six categories. The categories were selected in a way to have almost the same number of measurements (summer measurements were considered for PAR categories arrangements). The six PAR categories are <100, 100-350, 350-700, 700-1150, 1150-1500 & >1500 µmol photon^{-1} m^{-2} s^{-1}.

Summer NEE results are presented for the four sites in Figure 26 showing the distribution of the calculated CO_2 fluxes (NEE) over the six PAR categories and for each site in the study area. The figure shows a trend similar to 3.2.1 discussion for the all sites data, where NEE at lowest APR values <100 µmol photon^{-1} m^{-2} s^{-1} showing CO_2 release, suggesting low production (GPP) processes; then GPP starts to increase with PAR increase, resulting in higher CO_2 uptake. Also, as discussed for the whole site data in 3.2.1, production rate starts to be lower with PAR exceeding 750-1150 µmol photon^{-1} m^{-2} s^{-1} leading to less CO_2 uptake. This limiting PAR is related to photosynthesis light response curve (Spilatro, 1998) which is plant related factor.

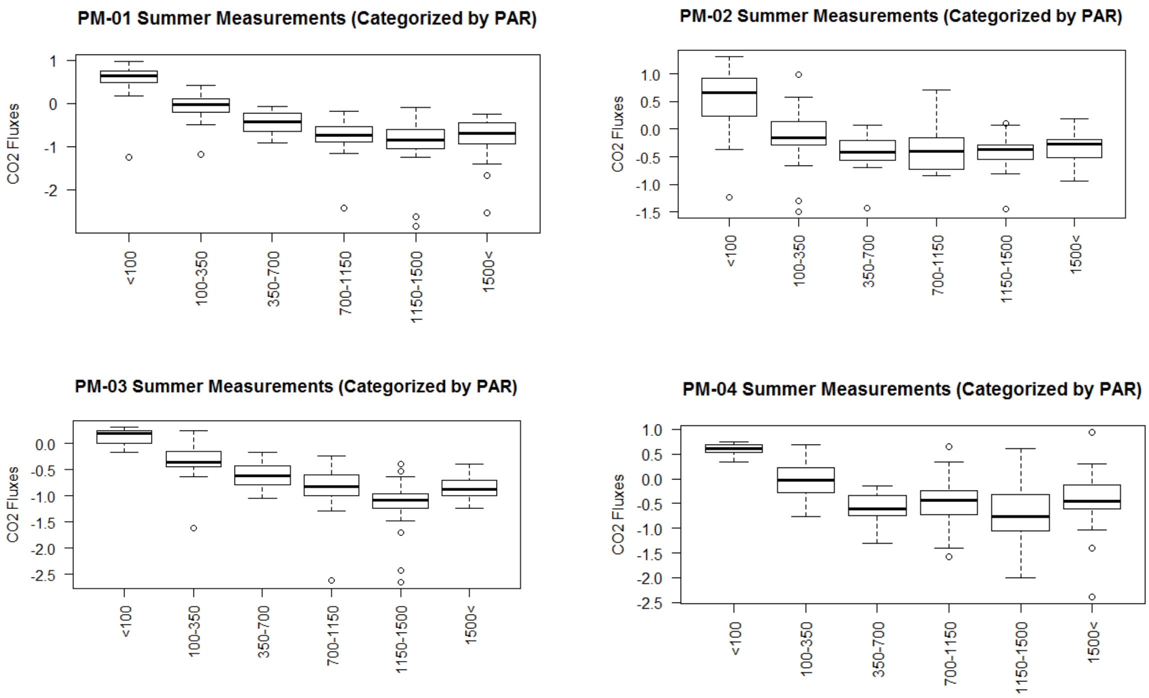

Figure 26: PAR Categorization and Distribution per Site (Summer Measurements) "CO_2 fluxes in (g m^{-2} h^{-1})"

Table 13 shows that at the lowest PAR <100 µmol $photon^{-1}$ m^{-2} s^{-1} sites PM1, PM2 & PM4 have CO_2 release fluxes while site PM3 shows low CO_2 release. But with PAR increase site PM3 has the highest CO_2 uptake compared with PM1, PM2 & PM4. Although sites PM2 & PM4 having the same plant species but with different size (PM4 plants are larger than PM2), site PM4 has higher NEE fluxes than PM2 suggesting that the size of biomass has an effect on the production process.

	Average NEE (g m^{-2} h^{-1}) - Summer Measurements			
PAR Cat.	**PM1**	**PM2**	**PM3**	**PM4**
< 100	0.514	0.525	0.110	0.582
100 - 350	-0.066	-0.150	-0.378	-0.056
350 - 700	-0.457	-0.379	-0.605	-0.612
700 - 1150	-0.679	-0.401	-0.792	-0.506
1150 - 1500	-0.779	-0.410	-1.055	-0.725
1500 <	-0.730	-0.348	-0.847	-0.363

Table 13: Average NEE per site and PAR category - Summer Measurements

Spring and autumn data are presented in Table 14, Figure 27 and Figure 28 which show similar trend for NEE with respect to PAR as in summer. Where, CO_2 release at low PAR, in spring the CO2 release is at PAR <100 µmol photon^{-1} m^{-2} s^{-1} for the four sites and in autumn for sites PM2 & PM4 it extends to PAR =100-350 µmol photon^{-1}m^{-2}s^{-1}. Suggesting that plant species has an effect on respiration process as PM2 & PM4 have the same species but with different plant size. Uptake increases with PAR increasing then with more PAR increase the production rate becomes lower and consequently less uptake. Autumn measurements for site PM3 shows that CO_2 uptake occurs also at the lowest PAR category. This could be explained by referring to Table 11 where it shows that in autumn at the same time (8:00) respiration fluxes are lower than GPP resulting in CO_2 uptake. This suggests that plant composition is also a factor affecting the ecosystem behaviour regarding CO_2 uptake/release.

	Average NEE (g m^{-2} h^{-1})							
	Spring Measurements				**Autumn Measurements**			
PAR Category	**PM1**	**PM2**	**PM3**	**PM4**	**PM1**	**PM2**	**PM3**	**PM4**
< 100	0.062	0.039	0.260	0.596	-	0.305	-0.157	0.496
100 - 350	-0.103	-0.108	-0.175	-0.315	-0.109	0.437	-0.187	0.483
350 - 700	-	-0.639	-0.408	-	-0.095	-0.135	-0.246	-0.089
700 - 1150	-	-0.335	-	-0.126	-0.010	-0.147	-0.241	-0.229
1150 - 1500	-0.183	-0.201	-0.420	-0.241	-	-	-	-
1500 <	-0.221	-0.251	-0.315	-0.345	-	-	-	-

Table 14: Average NEE per site and PAR category - Spring & Autumn Measurements

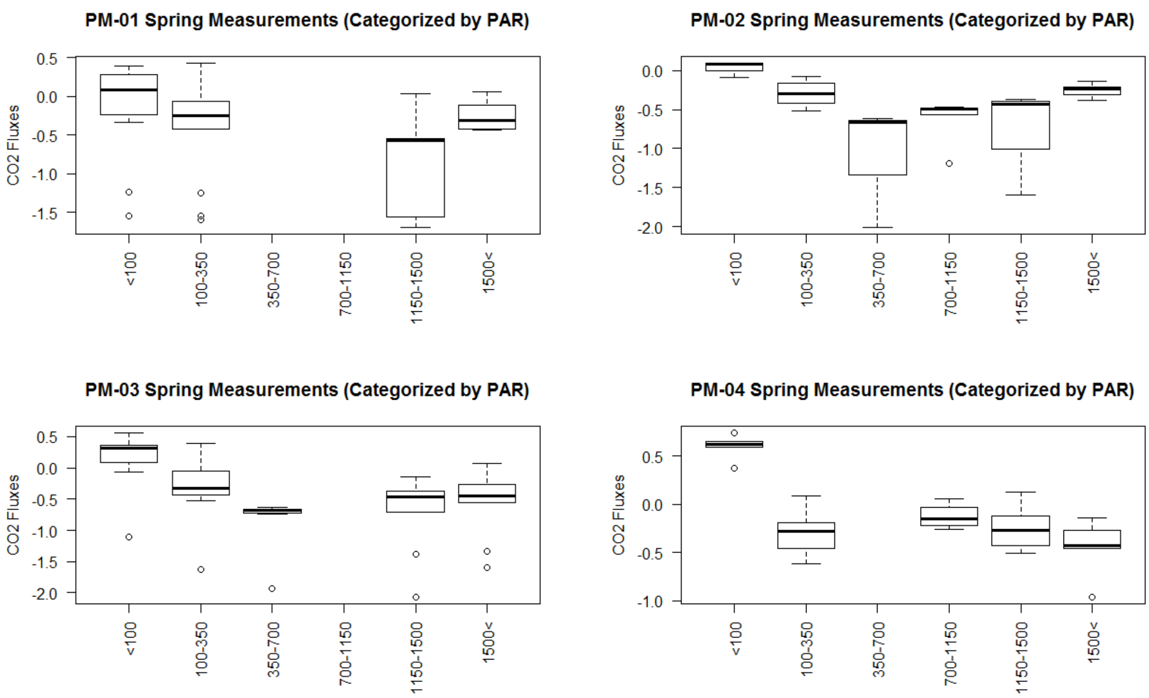

Figure 27: PAR Categorization and Distribution per Site (Spring Measurements) "CO_2 fluxes in (g m^{-2} h^{-1})"

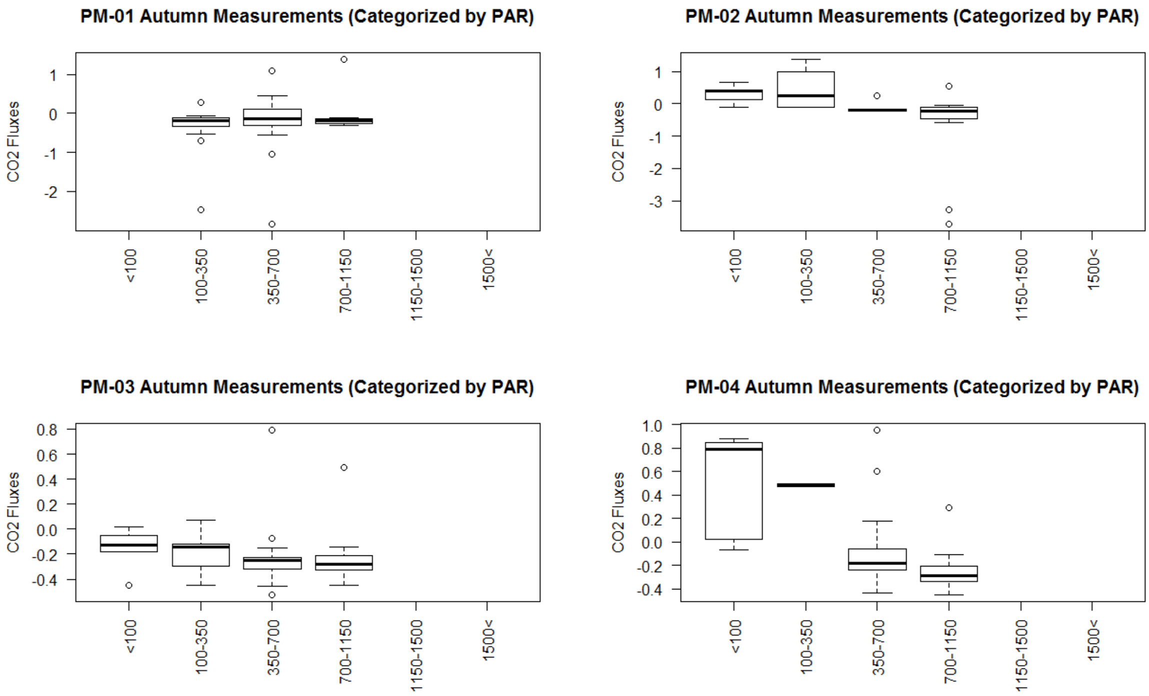

Figure 28: PAR Categorization and Distribution per Site (Autumn Measurements) "CO_2 fluxes in (g m^{-2} h^{-1})"

3.3.2 Soil Temperature Categorization

Soil temperature at 2cm depth were categorized into five categories (<15°C, 15-20°C, 20-25°C, 25-30°C and >30°C) in order to understand the relationship between respiration, production and temperature.

	Summer Measurements							
	Average NEE (g m^{-2} h^{-1})				**Average Day Time R_{eco} (g m^{-2} h^{-1})**			
Temp. Category	**PM1**	**PM2**	**PM3**	**PM4**	**PM1**	**PM2**	**PM3**	**PM4**
< 15	-	0.014	-0.087	0.495	-	0.742	-	0.796
15-20	-0.120	-0.047	-0.781	-0.757	0.587	0.639	0.537	0.527
20-25	-0.813	0.156	-0.978	-0.685	0.735	0.742	0.686	0.779
25-30	-0.380	-0.309	-0.786	-0.292	0.879	0.806	0.810	0.904
30 <	-0.642	-0.224	-0.730	-0.285	0.859	0.863	0.633	0.829

Table 15: NEE and R_{eco} distribution per temperature category and site (Summer Measurements)

Table 15 and Figure 29 are illustrating the relationship between NEE and soil temperature at 2cm for the four study sites. PM3 & PM4 show similar behaviour as carbon uptake increase with increasing temperature up to a transition point then uptake starts to reduce. For PM3 the transition temperature is 20-25°C and for PM4 is 15-20°C. Results show that PM4 starts at low temperature (<15°C) with CO_2 release this could be explained by considering that PM4 is showing the highest respiration fluxes between the four sites. Sites PM1 & PM2 showed less consistent relationship with temperature than PM3 & PM4.

The highest CO_2 uptake (negative NEE) was at PM3 (-0.978 g m^{-2} h^{-1}) followed by PM1 (-0.813 g m^{-2} h^{-1}), then PM4 (-0.757 g m^{-2} h^{-1}) and the lowest uptake was in PM2 (-0.309 g m^{-2} h^{-1}).

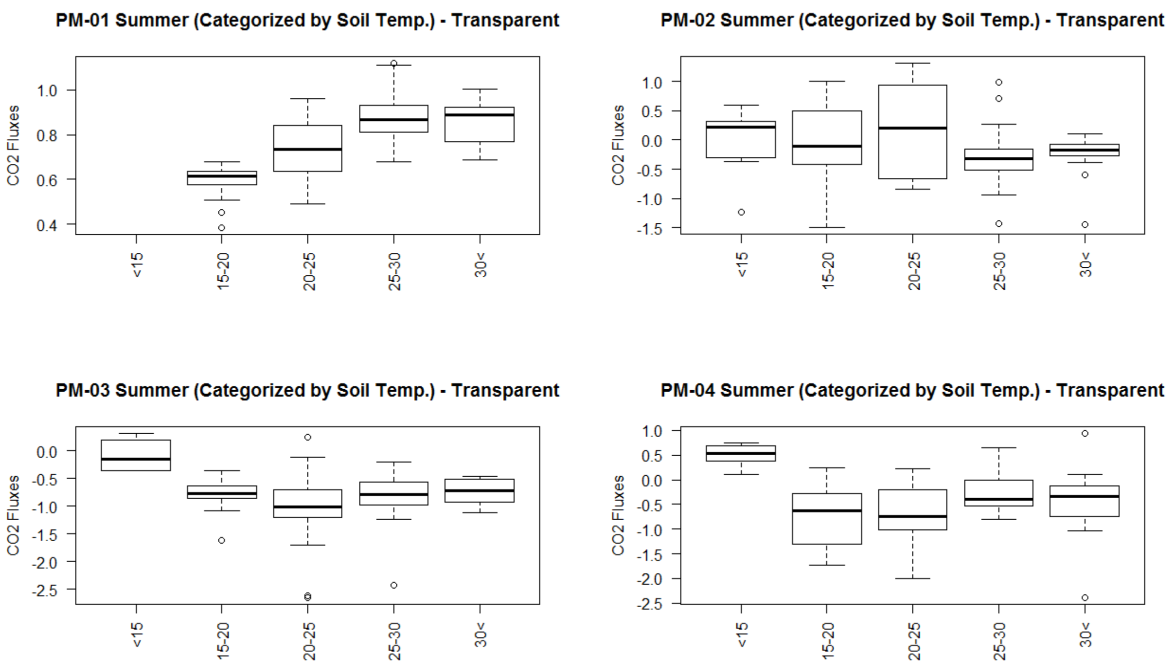

Figure 29: Soil Temp. Categorization and Distribution per Site (Summer - Transparent) "CO_2 fluxes in (g m^{-2} h^{-1})"

Average respiration measurements taken during day time of summer are presented in Table 15 and Figure 30 with respect to soil temperature at 2cm depth. The results show that similar trend for sites PM2 & PM4 where respiration at lowest temperature (<15°C) is higher than the second category (15-20°C) and then starts to increase with temperature increase, the increase continuous up to the highest temperature category (>30°C) where respiration starts to reduce again. Table 12 shows that temperature <15°C occurs at early morning (6:00), 15-20°C occur approximately between 7:00-9:00 and the highest temperature (>30°C) around 14:00.

Sites PM1 & PM3 showed similar trend like PM2 & PM4, but due to the absence of early morning respiration measurements the first respiration drop was not measured for both PM1 & PM3.

PM4 showed the highest respiration (0.904 g $m^{-2}h^{-1}$) followed by PM1 (0.879 g $m^{-2}h^{-1}$) then PM2 (0.863 g m^{-2} h^{-1}) and PM3 showed the lowest respiration (0.810 g m^{-2} h^{-1}).

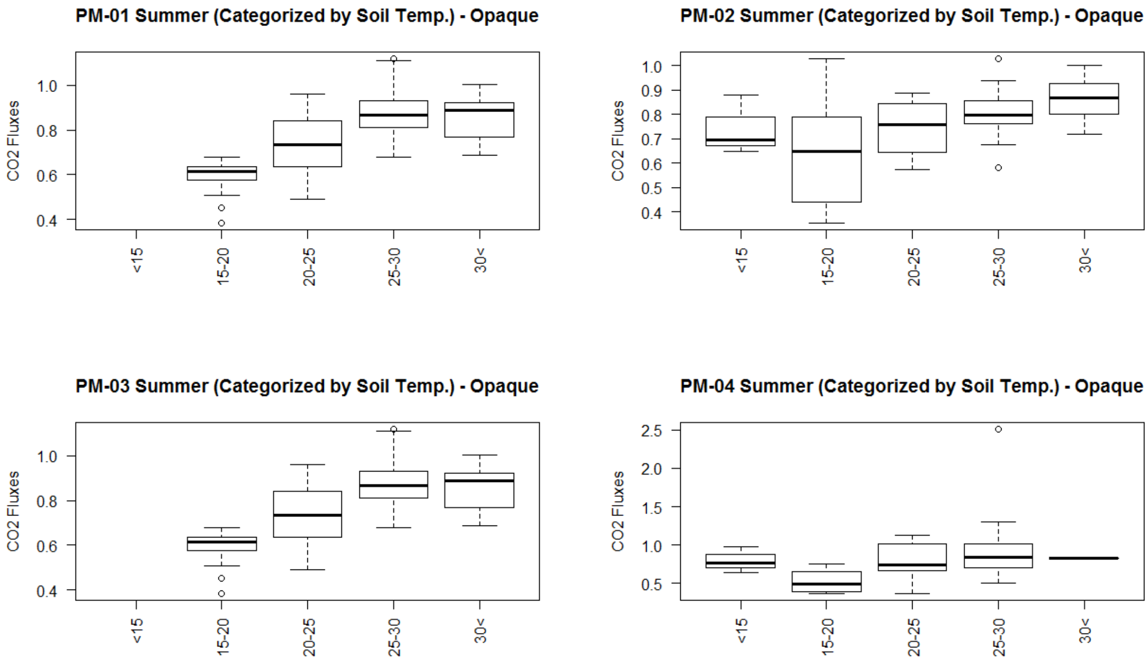

Figure 30: Soil Temp. Categorization and Distribution per Site (Summer - Opaque) "CO_2 fluxes in (g m^{-2} h^{-1})"

CO_2 fluxes distribution with respect to soil temperature at 2cm were also investigated for spring and autumn seasons and presented in Table 16.

	Average NEE (g m^{-2} h^{-1})							
	Spring Measurements				Autumn Measurements			
Temp. Category	**PM1**	**PM2**	**PM3**	**PM4**	**PM1**	**PM2**	**PM3**	**PM4**
< 15	-0.268	-0.460	-0.200	-0.352	-0.223	-0.155	-0.231	-0.024
15-20	-0.316	-0.198	-0.069	0.180	-	-	-	-
20-25	-0.283	-0.151	0.071	-0.156	-	-	-	-
25-30	-0.277	-	-0.322	-0.521	-	-	-	-
30 <	-	-	-	-	-	-	-	-

	Average Day Time R_{eco} (g m^{-2} h^{-1})							
	Spring Measurements				Autumn Measurements			
Temp. Category	**PM1**	**PM2**	**PM3**	**PM4**	**PM1**	**PM2**	**PM3**	**PM4**
< 15	0.276	0.338	0.328	0.375	0.134	0.670	0.210	0.272
15-20	0.354	0.348	-	-	-	-	-	-
20-25	-	-	-	-	-	-	-	-
25-30	-	-	-	-	-	-	-	-
30 <	-	-	-	-	-	-	-	-

Table 16: NEE and R_{eco} distribution per temperature category and site (Spring & Autumn Measurements)

Autumn measurements showed that PM2 has the highest respiration (0.670 g m^{-2} h^{-1}) and the lowest respiration for site PM1 (0.134 g m^{-2} h^{-1}), while sites M3 & PM4 respiration was almost the same order of magnitude (0.210 & 0.272 g m^{-2} h^{-1} respectively). On the other hand, PM4 showed the highest respiration in spring (0.375 g m^{-2} h^{-1}), PM1 the lowest (0.276 g m^{-2} h^{-1}). PM2 & PM3 was almost equal (0.338 and 0.328 g m^{-2} h^{-1} respectively).

Site PM3 has the highest CO_2 uptake in autumn (-0.231 g m^{-2} h^{-1}) and the lowest uptake was PM4 (-0.024 g m^{-2} h^{-1}). Spring measurements indicate the highest CO_2 uptake was in site PM4 (-0.521 g $m^{-2}h^{-1}$) then PM2 (-0.460 g $m^{-2}h^{-1}$) followed by PM3 (-0.322 g m^{-2} h^{-1}) and the lowest was in PM1 (-0.316 g m^{-2} h^{-1}). Also, the highest uptake in PM2 occurred at the lowest temperature category (<15°C), for PM1 at 15-20°C and for PM3 & PM4 at 25-30°C.

3.3.3 Comparison the Four Sites Summary

Ecosystem respiration (R_{eco}):

As discussed in 3.3.2, the four sites showed similar behaviour with temperature changes during summer day time measurements. However, the sites variability affected the measured respiration fluxes.

PM4 showed the highest respiration, supported by comparing the NEE values in Table 15 showing that PM4 at the lowest temperature category (<15°C), which occurs as per Table 12 at early morning 6:00 with low PAR values (i.e. no production process), releases CO_2 (0.904 g m^{-2} h^{-1}). Spring measurements also showed that PM4 has the highest respiration fluxes but in autumn PM4 was not the highest one. This suggests that PM4 respiration process is much slower at low temperature, as shown in Table 12 for autumn temperatures and in Table 15 for NEE at the lowest temperature category.

Although, sites PM3 & PM4 are almost in the same area but PM4 showed the highest respiration during summer and PM3 the lowest respiration. By considering water levels as shown in Table 17; it could be noted that although water level in PM3 is lower than PM4 in the three seasons but this did not affect respiration order between the PM3 & PM4. All of this supports that plant composition affects respiration process with less impact of water level.

PM1 showed higher respiration than PM2 in summer, but in spring and autumn this relationship was reversed (as PM2 was higher in respiration than PM1). Table 17 shows that water level for both PM1 & PM2 over the three seasons.

	Water Level (cm)			
	PM1	**PM2**	**PM3**	**PM4**
Spring	-6.8	-8.8	-15.83	-12.83
Summer	-11.3	-12.76	-19.89	-16.36
Autumn	-11.04	-10.21	-20.5	-15.14

Table 17: Average water level at the four sites

Water level in autumn is lower than in spring which might suggest that it might be expected to have higher respiration fluxes due to the increase in the aerobic zone. But the results do not show that, as respiration in spring is higher than in autumn.

Gross Primary Production (GPP):

Table 18 and Table 19 are showing the calculated GPP seasonal distribution over the temperature categories per site. PM3 shows the highest production (-1.664 g m^{-2} h^{-1}) in summer, then PM1 (-1.548 g m^{-2} h^{-1}) followed by PM4 (-1.464 g m^{-2} h^{-1}) and the lowest production in PM2 (-1.115 g m^{-2} h^{-1}).

Site PM2 had the highest production in both spring and autumn (-0.768 and -0.825 g m^{-2} h^{-1} respectively). The lowest production in spring was PM3 (-0.528 g m^{-2} h^{-1}) and in autumn was PM4 (-0.296 g m^{-2} h^{-1}).

	Summer Measurements			
	Calculated GPP (g m^{-2} h^{-1})			
Temp. Category	**PM1**	**PM2**	**PM3**	**PM4**
< 15	-	-0.728	-	-0.301
15-20	-0.707	-0.686	-1.318	-1.284
20-25	-1.548	-0.586	-1.664	-1.464
25-30	-1.259	-1.115	-1.596	-1.196
30 <	-1.501	-1.087	-1.363	-1.114

Table 18: Calculated GPP distribution per temperature category and site (Summer Measurements)

	Calculated GPP (g m^{-2} h^{-1})							
	Spring Measurements				**Autumn Measurements**			
Temp. Category	**PM1**	**PM2**	**PM3**	**PM4**	**PM1**	**PM2**	**PM3**	**PM4**
< 15	-0.544	-0.798	-0.528	-0.727	-0.357	-0.825	-0.441	-0.296
15-20	-0.670	-0.546	-	-	-	-	-	-
20-25	-	-	-	-	-	-	-	-
25-30	-	-	-	-	-	-	-	-
30 <	-	-	-	-	-	-	-	-

Table 19: Calculated GPP distribution per temperature category and site (Spring & Autumn Measurements)

It could me noted that summer has the highest GPP values compared with spring and autumn is the lowest GPP values. Except for site PM2 where summer is lower, even it might be noted that the three seasons are almost of the same order of magnitude. Site PM2 almost has the similar GPP fluxes in the three seasons which might suggest that the plant composition in this site is less sensitive to seasonal changes than the other three sites. However, this is not the same in site PM4 which has the same plant composition as site PM2 (except plants in PM4 are larger than in PM2).

Such production variability supports that different plant composition have different production rates at the different climatic changes.

Net Ecosystem Exchange (NEE):

At low temperature production processes (GPP) are higher than ecosystem respiration (R_{eco}) processes, by temperature increase both production and respiration increase but considering respiration is a slow process, GPP fluxes are higher than R_{eco} fluxes resulting in CO_2 uptake (negative NEE). At certain temperature and PAR, production starts to get lower and respiration continue to increase with temperature increase resulting in reduction in NEE (i.e. CO_2 uptake becomes lower and in some measurements, turn to CO_2 release).

As presented in Table 15 and Table 16, PM3 showed the highest CO_2 uptake in summer (-0.978 g m^{-2} h^{-1}) which at the same time has the highest production (-1.664 g m^{-2} h^{-1}) even that PM3 is not the highest site in respiration.

In spring, the highest CO_2 uptake was in site PM4 (-0.521 g m^{-2} h^{-1}) but the PM2 was the highest in production (-0.768 g m^{-2} h^{-1}) and PM4 was the highest in respiration (0.375 g m^{-2} h^{-1}).

PM3 was the highest CO_2 uptake in autumn (-0.231 g m^{-2} h^{-1}) and PM2 was the highest in production (-0.825 g m^{-2} h^{-1}) and also the in highest respiration (0.670 g m^{-2} h^{-1}).

Such differences suggest that the ecosystem behaviour as a CO_2 sink or source is affected by the combination between plant composition and seasonal variabilities work.

3.4 Comparison within the Site

In this study, three replicate frames were used in each site to provide more comparable data for field measurements. Due to the fact that the biomass and ground surface topography as well as frame penetration in the soil are not completely identical in each study site; these frames variabilities resulting in expected differences within each site. Annex 2 – Sites' Frames Results, provides a comparison of the seasonal average fluxes, during day time, between the frames in each site. Night time respiration was not modelled up to the frames level (only up to the site level).

3.4.1 Site PM1 Frames

As indicated in Table 20, frame PM1-2 showed, for NEE and day time respiration measurements, less correlation than PM1-1 & PM1-3 with respect to PAR and soil temperature at 2cm depth. On the other hand, PM1-1 & PM1-3 had almost the same correlation coefficients with respect the same parameters. This suggests that the vegetation density of PM1-2 is different than in PM1-1 & PM1-3.

	PM1-1	PM1-2	PM1-3
NEE Correlation with PAR	-0.504	-0.675	-0.627
NEE Correlation with Soil Temperature at 2cm depth	-0.295	-0.187	-0.215
R_{eco} Correlation with Soil Temperature at 2cm depth	0.943	0.864	0.928

Table 20: Site PM1 Frames correlation coefficients

3.4.2 Site PM2 Frames

As shown in Table 21, respiration in frame PM2-1 is significantly less correlated with soil temperature than in PM2-2 & PM2-3. Additionally, NEE in frames PM2-1 & PM2-2 have less correlation with soil temperature than PM2-3. The comparison of NEE correlation with PAR showed that PM2-1 & PM2-2 has almost the same order of magnitude and less than PM2-3. This might suggest that PM2-1 & PM2-2 have the same above ground biomass compared with PM2-3. The low correlation of respiration in PM2-1 compared with PM2-1 & PM2-3, suggests that additional factors other than the differences in vegetation density might also have an impact. These factors could be resulting from differences in below ground ecosystem or the measurements used.

	PM2-1	PM2-2	PM2-3
NEE Correlation with PAR	-0.364	-0.434	-0.634
NEE Correlation with Soil Temperature at 2cm depth	0.013	-0.055	-0.187
R_{eco} Correlation with Soil Temperature at 2cm depth	0.012	0.694	0.820

Table 21: Site PM2 Frames correlation coefficients

3.4.3 Site PM3 Frames

As illustrated in Table 22, no significant correlation variability between the frames suggesting that plant composition and vegetation density in the three frames are almost similar.

	PM3-1	PM3-2	PM3-3
NEE Correlation with PAR	-0.430	-0.685	-0.548
NEE Correlation with Soil Temperature at 2cm depth	-0.320	-0.492	-0.477
R_{eco} Correlation with Soil Temperature at 2cm depth	0.827	0.819	0.740

Table 22: Site PM3 Frames correlation coefficients

3.4.4 Site PM4 Frames

Table 23 shows that site PM4 frames are almost similar and the variations in correlation coefficients could be explained in the view of the plant composition variability between each frame.

	PM4-1	PM4-2	PM4-3
NEE Correlation with PAR	-0.334	-0.483	-0.522
NEE Correlation with Soil Temperature at 2cm depth	-0.183	-0.230	-0.302
R_{eco} Correlation with Soil Temperature at 2cm depth	0.532	0.739	0.602

Table 23: Site PM4 Frames correlation coefficients

3.5 Eddy Covariance Results Comparison

As mentioned in 2.1, CO_2 measurements have more than one approach, the closed chamber the one used in this study and the eddy covariance which was used in the same study area. A comparison was made between the results of the fluxes measured and calculated under this study with the same as measured by the eddy covariance approach.

	Eddy covariance			Closed Chamber			Chamber/Eddy %		
Average values of:	**Spring**	**Summer**	**Autumn**	**Spring**	**Summer**	**Autumn**	**Spring**	**Summer**	**Autumn**
Day time soil temperature (°c)	15.37	21.58	12.27	16.16	24.09	11.70	105%	112%	95%
Night time soil temperature (°C)	11.92	17.33	9.26	13.16	15.64	11.80	110%	90%	127%
PAR (µmol photon^{-1} m^{-2} s^{-1})	534.30	754.49	396.29	550.36	926.00	493.23	103%	123%	124%
Day time NEE (g m^{-2} h^{-1})	-0.162	-0.251	-0.331	-0.294	-0.427	-0.170	181%	170%	51%
R_{eco} (day time from Chamber) (g m^{-2} h^{-1})	0.703	1.327	0.498	0.327	0.767	0.359	47%	58%	72%
R_{eco} (calculated from Chamber) (g m^{-2} h^{-1})	0.703	1.327	0.498	0.394	0.468	0.353	56%	35%	71%

Table 24: Eddy Covariance results comparison

Table 24 compares the field parameters measured by eddy tower and the GERD including soil temperature at 2cm depth during day time measurements; the estimated night time soil temperature at 2cm depth as explained in 3.6.2 & the temperature night measurements by eddy tower; measured PAR; measured NEE by both approaches; and respiration as measured during day time chamber measurements, eddy tower during night time & as estimated by the model explained in 3.6.2.

The comparison showed some deviations between both approaches, chamber measurements provided higher results than eddy covariance in temperature, PAR and NEE measurements. While respiration measurements made by eddy approach were higher than chamber approach. With the same order of magnitude of the percentage of the measured and estimated respiration percentages.

3.6 CO_2 Balance for the Ecosystem

3.6.1 Soil and Air Temperature Correlation

In the analysis, the relationship between CO_2 fluxes and only soil temperature at 2 cm depth were investigated. Table 25 and Figure 31 show that air temperature and soil temperature at 2, 5 & 10 cm are strongly correlated. Which allows to expand the conclusions related to CO_2 fluxes and soil temperature at 2cm to cover also air temperature and soil profile temperature (till the measured depth 10cm). However, soil temperature ate 2 & 5 cm depth are showing higher correlation than the 10cm depth. This might suggest that the effect of near surface temperature is more significant.

	Correlation with	**Correlation coefficient (r)**		
		Spring	**Summer**	**Autumn**
Soil Temperature at 2cm depth	Air Temperature	0.95	0.92	-0.12
Soil Temperature at 5cm depth	Soil Temperature at 2cm depth	0.93	0.94	0.90
Soil Temperature at 10cm depth	Soil Temperature at 5cm depth	0.81	0.80	0.94

Table 25: Temperature Correlation Matrix

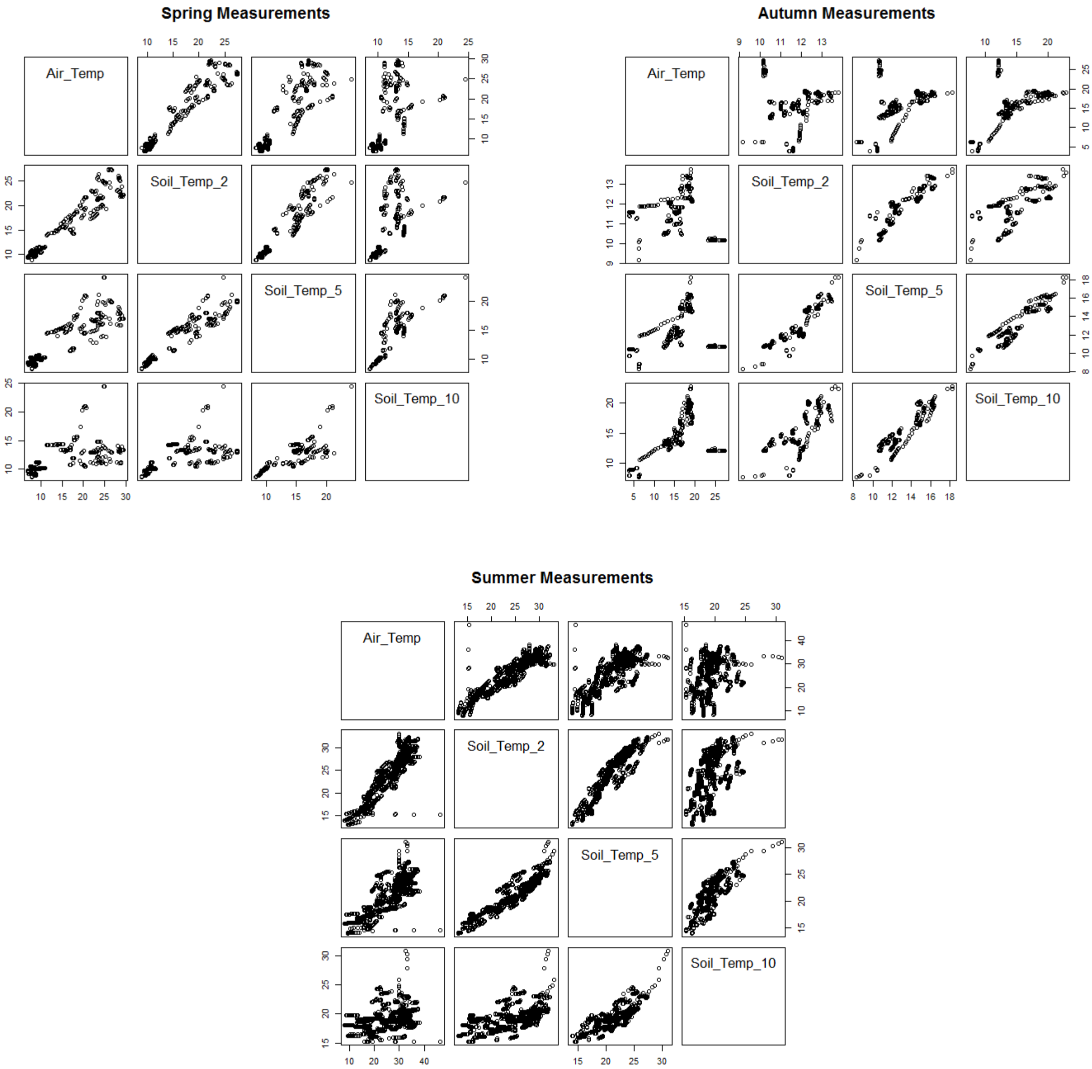

Figure 31: Temperature Correlation Matrix

3.6.2 Ecosystem Respiration (R_{eco})

As discussed in 3.2.2, ecosystem respiration, measured during day time, showed good correlation with temperature (r= 0.763) where summer measurements indicated higher correlation than spring and autumn which showed the lowest correlation (seasonal correlation values were; r=0.445, 0.318 and 0.084 for summer, spring and autumn respectively). On the other hand, as discussed in 3.3.2, correlation analysis between respiration and temperature for the four study sites indicated high correlation; for site PM1 (r= 0.8102), PM2 (r= 0.5084), PM3 (r= 0.5816) and PM4 (r= 0.4129).

Using "R" software and in order to estimate the overall CO_2 balance for this ecosystem, a model was created to estimate the whole day respiration (including night and day time) and to estimate respiration for the whole seasons' days. This provide a complete overview for the ecosystem respiration over the seasons (winter is also included in this estimate) and for the four study sites.

Based on air temperature/soil correlation presented in 3.6.1, the model was made to calculate R_{eco} as a function of soil temperature at 2cm depth.

Linear and exponential relationship were investigated and the analysis indicated that R^2 was 0.5813 and 0.5303 for the linear and exponential equations respectively. Therefore, the linear equation was selected (as shown in Figure 23) and the model equation is: "$R_{eco} = a + b * T$"

Where:

- T = soil temperature at 2cm depth
- a & b = constants

Seasonal models were tested but the R^2 values were low (R^2 for spring, summer & autumn were 0.0737, 0.1942 & -0.02043 respectively).

Accordingly, the respiration model will cover each individual site (PM1, PM2, PM3 & PM4) to study the different behaviour for each site regarding this issue.

Table 26 shows the model parameters for the whole study area and for each site of the four sites.

	a	b	R^2
PM1	-0.176±0.044	0.037±0.002	0.8102
PM2	0.144±0.061	0.024±0.003	0.5084
PM3	-0.032±0.074	0.029±0.003	0.5816
PM4	0.086±0.100	0.028±0.004	0.4129

Table 26: Respiration model parameters

For the purpose of this model and in order to have a complete temperature data set, temperature measured by Eddy measurement station was used as shown in Table 31 in Annex 3 – NEE and Reco Models.

3.6.3 Net Ecosystem Exchange (NEE)

Following the same approach for respiration model, day time NEE was also modelled. This was based on the discussion made in 3.2.1, where in which NEE showed correlation with PAR.

A model was created to estimate day time NEE for the whole seasons days and to provide an estimate even for the not measured days. This provide a complete overview for the day time NEE over the seasons (winter is also included in this estimate) and for the four study sites.

A simple model based on linear relationship used to model NEE with respect to PAR for each individual site (PM1, PM2, PM3 & PM4) to study the different behaviour for each site regarding this issue and the model equation is: “NEE = a + b * PAR”

Where:

- a & b = constants

Table 27 shows the model parameters for the whole study area and for each site of the four sites.

	a	b	R^2
PM1	9.553e-02± 8.181e-02	-3.980e-04±8.599e-05	0.04951
PM2	1.836e-01±5.340e-02	-4.789e-04±5.712e-05	0.2117
PM3	-1.882e-01±5.022e-02	-4.763e-04±4.931e-05	0.252
PM4	2.691e-02±6.133e-02	-3.815e-04±5.468e-05	0.1681

Table 27: NEE model parameters

For the purpose of this model and in order to have a complete PAR data set, PAR measured by Eddy measurement station was used as shown in Table 31 in Annex 3 – NEE and Reco Models.

From Table 27, it could be noted that the model equations have low R^2 value. This could be due to the variability in PAR depending on weather conditions changes (such as cloud cover).

In order to integrate the production processes within the overall NEE model, sun rise and sun set hours over seasons were estimated as shown in Table 28.

	Sun Rise	Sun Set
Spring	6:00	19:00
Summer	5:00	21:00
Autumn	6:00	18:00
Winter	7:00	17:00

Table 28: Estimated Sun Rise and Sun Set

3.6.4 Ecosystem CO_2 Balance

Based on NEE and R_{eco} models (as presented in 3.6.2 and 3.6.3 above), the hourly fluxes for GPP, R_{eco} and NEE were estimated as shown in Table 32, Table 33 and Table 34 in Annex 3 – NEE and Reco Models. Accordingly, the total seasonal fluxes for each of the study sites were estimated as shown in Table 29.

During modelling some adjustments were made to the calculated fluxes as outlined below:

- GPP fluxes with positive values were eliminated since all GPP values should be negative values. Such values were occurred at very low PAR values (specially in winter calculated fluxes)
- Similarly, R_{eco} fluxes with negative values were eliminated since all R_{eco} values should be positive values. Such values occurred in winter calculated fluxes (specially at site PM1), this could be either due to the low temperature in winter season did not fit with the model equation

	Total daily [g m^{-2} d^{-1}]			Total seasonal [kg m^{-2} $sesons^{-1}$]			Total annual [kg m^{-2}yr-^{1}]		
	GPP	R_{eco}	NEE	GPP	R_{eco}	NEE	GPP	R_{eco}	NEE
PM1									
Spring	-7.536	8.393	0.857	-0.693	0.772	0.079	-2.209	2.463	0.254
Summer	-12.877	13.393	0.516	-1.185	1.232	0.047			
Autumn	-3.493	5.039	1.546	-0.318	0.459	0.141			
Winter	-0.144	0.000	-0.144	-0.013	0.000	-0.013			
PM2									
Spring	-8.554	11.696	3.142	-0.787	1.076	0.289	-2.535	3.761	1.227
Summer	-13.046	14.960	1.914	-1.200	1.376	0.176			
Autumn	-4.947	9.508	4.561	-0.450	0.865	0.415			
Winter	-1.080	4.930	3.849	-0.097	0.444	0.346			
PM3									
Spring	-12.365	9.141	-3.224	-1.138	0.841	-0.297	-3.854	2.725	-1.129
Summer	-18.112	13.069	-5.042	-1.666	1.202	-0.464			
Autumn	-8.199	6.506	-1.693	-0.746	0.592	-0.154			
Winter	-3.373	0.996	-2.377	-0.304	0.090	-0.214			
PM4									
Spring	-10.008	11.576	1.568	-0.921	1.065	0.144	-3.077	3.639	0.562
Summer	-15.045	15.343	0.299	-1.384	1.412	0.027			
Autumn	-6.388	9.048	2.660	-0.581	0.823	0.242			
Winter	-2.117	3.763	1.647	-0.190	0.339	0.148			

Table 29: Seasonal and annual CO_2 balance per square meter

(M. Minke et al, 2015) results showed that fluxes are varied significantly between the sites; R_{eco} ranged from 232 gCO_2-C m^{-2} yr^{-1} (0.851 kg m^{-2} yr^{-1}) to 1270 gCO_2-C m^{-2} yr^{-1} (4.661 kg m^{-2} yr^{-1}); GPP from -302 gCO_2-C m^{-2} yr^{-1} (-1.108 kg m^{-2} yr^{-1}) to -2267 gCO_2-C m^{-2} yr^{-1} (-8.320 kg m^{-2} yr^{-1}); and NEE from 216 gCO_2-C m^{-2} yr^{-1} (0.793 kg m^{-2} yr^{-1}) to -1175 gCO_2-C m^{-2} yr^{-1} (-4.312 kg m^{-2} yr^{-1}).

(O. Koch et al, 2008) discussion indicated annual carbon sinks for the study sites with NEE "-53 gC m^{-2} yr^{-1} (-0.195 kg m^{-2} yr^{-1}) to -138 gC m^{-2} yr^{-1} (-0.506 kg m^{-2} yr^{-1}). The discussion also concluded that no consistent pattern in the alpine region with regards to carbon balance.

This could explain the variability in the results, nevertheless the modelled annual fluxes (Table 29) could be considered in the same order of magnitude with the previous results.

Comparing modelled respiration fluxes of PM2 and PM4 show that PM4 has higher respiration rates in summer than PM2 (1.412 kg m^{-2} yr^{-1} and 1.376 kg m^{-2} yr^{-1} respectively), whereas PM2 demonstrates higher respiration in the other three seasons (spring: PM2 1.076 kg m^{-2} yr^{-1} & PM4 1.065 kg m^{-2} yr^{-1}; autumn: PM2 0.85 kg m^{-2} yr^{-1} & PM4 0.823 kg m^{-2} yr^{-1}; and winter: PM2 0.444 kg m^{-2} yr^{-1} & PM4 0.339 kg m^{-2} yr^{-1}). Taking into consideration that study sites PM4 and PM2 feature the same plant composition with larger *Pinus mugo* individuals at PM4 indicate the impact of aboveground biomass size and suggest that conifers at summer reach their maximum development (the difference between PM2 & PM4 respiration in the other seasons are much lower than the difference in Summer).

Same as for soil respiration, PM2 and PM4 modelled production fluxes of PM2 and PM4 show that PM4 has higher production in summer than PM2 (-1.384 kg m^{-2} yr^{-1} and -1.200 kg m^{-2} yr^{-1} respectively). On the contrary to respiration, PM4 is also higher in production than PM2 in the other three seasons (spring: PM2 -0.787 kg m^{-2} yr^{-1} & PM4 -0.921 kg m^{-2} yr^{-1}; autumn: PM2 -0.450 kg m^{-2} yr^{-1} & PM4 -0.581 kg m^{-2} yr^{-1}; and winter: PM2 -0.097 kg m^{-2} yr^{-1} & PM4 -0.190 kg m^{-2} yr^{-1}).

The modelled NEE rates demonstrate that site PM3 features highest CO_2 annual production (-3.854 kg $m^{-2}yr^{-1}$) and PM3 has low annual respiration (2.725 kg m^{-2} yr^{-1}) resulting in highest carbon sink of all investigated study sites (-1.129 kg m^{-2} yr^{-1} – GPP/R_{eco} is 141%). On the other hand, PM2 showed low CO_2 annual production (-2.535 kg m^{-2} yr^{-1}) and highest annual respiration (3.761 kg m^{-2} yr^{-1}) resulting in the lowest NEE (1.227kg m^{-2} yr^{-1} – GPP/R_{eco} is 67%). These results suggest that plant composition has a major effect on the peat status (as a CO_2 sink/source) as discussed in detail in 4.3.3 below.

PM1 is almost neutral with tendency to act as a CO_2 source, the annual production and respiration are almost close to each other (GPP: -2.209 kg m^{-2} yr^{-1} and R_{eco}: 2.463 kg m^{-2} yr^{-1} – GPP/R_{eco} is 90%).

CHAPTER 4 – DISCUSSION

4.1 Ecosystem Respiration (R_{eco})

4.1.1 Seasonal Variability

The four study sites feature the highest respiration fluxes (Table 29) in summer followed by spring then autumn and winter was the lowest. This observation is in line with a study was made by (Bogdan H. Chojnicki et al, 2009), who observed that the highest rates of ecosystem respiration occurred during summer and is explainable by the highest temperature and the aboveground biomass reaching the maximum stage development. (Manuel Acosta et al, 2017) also, indicated the highest respiration of four study sites in summer.

4.1.2 Water Table Dependency

Results depicted in Table 17 demonstrate that water table in spring is higher than in summer and autumn, which is expected since groundwater starts to accumulate from the rain season in summer followed by less water losses due to low evapotranspiration in autumn and winter leading to higher water table in spring. Lowered water table levels increase the unsaturated zone (acrotelm), consequently enhance the aerobic decomposition rates, thus resulting in higher belowground respiration fluxes. Summer results show highest respiration rates and lowest water table at the same time; however, this is not valid for measurements in spring and autumn. Autumn measurements show lower water tables compared to spring, but results indicate respiration rates being higher in spring than in autumn, this is explained by considering that plant activity are higher in spring compared to autumn.

Water table depth may have a significant effect on belowground respiration, since lowered water tables enlarge the aerobic zone and leads to faster decomposition rates. However, during the sampling periods of the respective seasons, water tables did not change much, so that these effects could not be revealed with our sampling design and may be overlaid by other effects.

This could be explained with the assumption that soil respiration (rather) depends on temperature than on water table depths (F.J.W. Parmentier et al, 2008). The authors conclude that the effect of water table changes depend on soil water retention characteristics. In case of high water retention, the effect of water level fluctuations is less. The high-water retention leads to less changes in water content in the root zone and soil water suction does not become critical for plants. On the other hand, respiration in soil with low water retention is directly affected by water level fluctuation. Similarly, (O. Koch et al, 2008) results show the significant dependence of respiration on water-filled pore space, which depends on soil water retention characteristics dependant.

According to (F.J.W. Parmentier et al, 2008) conclusion, soil water retention characteristics define the controlling factors for ecosystem respiration. In soils with high water retention, respiration is more controlled by temperature than by water level fluctuations and in low water retention, water level fluctuations have a controlling effect.

The existence of *Sphagnum* at all study sites might also explain the low dependency on water table, since *Sphagnum* features specific characteristics, which make it much more resistant to decomposition (F. St-Hilaire et al, 2010) (Lindsay, 2010), even under aerobic conditions. *Sphagnum* manipulate the chemical environment by changing pH of its micro-environment to partially paralysing the decomposition microorganisms. Additionally, the chemical composition of *Sphagnum* can block nitrogen pathways in the microorganisms (Lindsay, 2010). As well as high water retention capacity of *Sphagnum* and the peatland of this study demonstrates a nearly complete *Sphagnum* cover

Similarly, (Manuel Acosta et al, 2017) discussed that some sites show weak relationship between R_{eco} and water table depth and other sites show strong relationship. This confirms the importance of plant community on respiration, especially the high-water content in *Sphagnum mosses* and its ability to retain water and reduce the impact of water table fluctuations.

4.1.3 Temperature Dependency

Average daytime respiration rates show that respiration is lowest at low temperature categories and increase with rising temperatures. This increase continues up to the highest temperature category (>30°C), then respiration starts to reduce again as a result of the plants protection activity against high temperatures by closing stomata to stop water losses. At the same time and for the same reason, we can observe that GPP fluxes are getting lower at high temperatures.

By comparing the modelled respiration fluxes (Table 34), we observed that the daily temperature variability results in diurnal pattern of respiration rates. The highest respiration fluxes occurred around 14:00 when highest temperatures are recorded. Lowest fluxes occurred at 5:00 (in spring, summer & autumn) and in winter at 1:00.

Respiration diurnal pattern was similar to the pattern presented by (Manuel Acosta et al, 2017): respiration starts with low fluxes in the early morning and increase gradually reaching the peak around early afternoon (same as our results), then starts to decrease.

This diurnal respiration pattern supports the strong positive correlation of ecosystem respiration (R_{eco}) with temperature changes over the day time and seasonal variabilities. This could be supported by (P. C. Stoy et al, 2013), since biological activities are affected by climate weekly and monthly variability. Our results are also in line with (Bogdan H. Chojnicki et al, 2009), who concluded that vegetation structure and water depth play important roles in CO_2 fluxes distribution. Nevertheless, air temperature has been identified as decisive factor determining the daily and seasonal variability in ecosystem respiration rates. Similarly, (O. Koch et al, 2008) study showed soil respiration being closely linked to soil temperature.

4.2 Gross Primary Production (GPP)

4.2.1 Seasonal Variability

Our results suggest that Gross Primary Production (Table 29) is highest in summer, followed by spring, then autumn and finally much lower values in winter at all four study sites. This suggests that photosynthetic carbon fixation is mainly governed by seasonal changes in photosynthetically active radiation. This is also supported by (Strack M. et al, 2008); seasonal variability affects productivity, warmer temperatures result in longer growing seasons. Also, biomass production and respiration are affected by vegetation community and available nutrients leading at the end to define carbon sequestration status.

4.2.2 PAR Dependency

Table 32 demonstrates modelled primary production following PAR changes supporting the direct relationship between gross primary production and PAR. This is similar to the findings regarding the significant dependence of NEE on PAR (O. Koch et al, 2008).

Our results also show that at high PAR values the change rate in production flux is getting less and at low PAR values is getting high. This could be explained with photosynthesis light response curve, this curve show the efficiency at which light is utilized by photosynthesis (Spilatro, 1998) as shown in Figure 32.

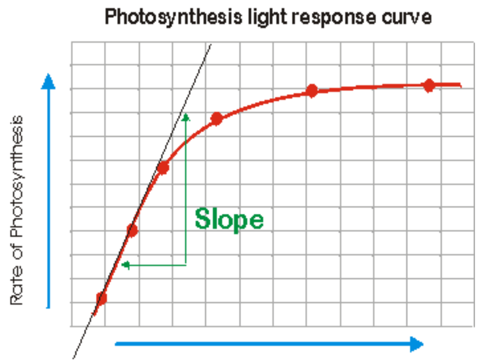

Figure 32: Photosynthesis light response curve

The above pattern occurs in the four study sites, but with different magnitudes as a result of the different plant compositions at the sites.

During summer, NEE is the highest between the seasons, even at the same PAR category (as shown in Table 10). This reveals, even though PAR is a major factor affecting GPP but also the seasonal climatic variability need to be considered.

The highest modelled GPP occurred around 13:00 in the four seasons which is almost corresponding with the highest recorded PAR.

4.2.3 Temperature Dependency

Photosynthetic carbon fixation showed dependency to temperature variability similar to respiration dependency. This also could be observed in warmer seasons featuring higher GPP than colder seasons. Since warmer temperature results in longer growing seasons (Strack M. et al, 2008).

4.3 Net Ecosystem Exchange (NEE)

4.3.1 Day-time NEE

In Day-time NEE (Table 11 and Table 33) illustrate that the system starts as CO_2 source and with PAR and temperature (as shown in Table 12 and Table 31) the CO_2 uptake increases following the same GPP trend). This NEE day-time pattern is maintained over the study seasons but with different magnitudes. Following the discussion in 4.2.1, measured day-time NEE illustrates higher CO_2 uptake in summer than in spring, autumn results showed the lowest values of measured day-time CO_2 uptake and is switching to CO_2 release.

(Manuel Acosta et al, 2017) results presented similar conclusion, NEE in the early morning is the highest and decreases till early afternoon and starts to increase again. Also, (Manuel Acosta et al, 2017) summer measurements showed the highest NEE compared with the other study seasons.

This could be explained by considering two issues; Firstly, the plant production rate is getting higher in summer than in spring as a result of longer growing seasons with warmer temperatures in addition to longer day hours (Strack M. et al, 2008). Secondly, in peatlands the growth rate is much faster than the respiration rate as discussed by (Lindsay, 2010). Peat rich in *Sphagnum* tends to be less decomposed than other peat forming plants, additionally other peat forming plants decompose at slow rate as long as the anaerobic conditions exists. Leaving the high decomposition rate in the aerobic layer, however the discussion in 4.1.2 indicated that the study sites are showing low dependency on water table.

4.3.2 Total NEE

From Table 29, it could be noted that respiration rates for PM2 & PM4 are almost in the same order of magnitude (with small differences compared with the differences with PM1 & PM3). It also shows that PM1 & PM3 are the lowest in respiration. Also, in PM1 & PM3 winter results show no respiration were calculated for PM1 and a very low value for PM3, this could be due to winter low temperature could not fit in the model for these two sites. However, PM2 & PM4 have the highest seasonal respiration as well as in winter, which under the same low temperature as in PM1 & PM3, the respiration in PM2 & PM4 were considerably higher.

The calculated results show also that summer have the highest respiration rate than spring and autumn, which is matching the discussion in 3.2.2 related to having higher day time respiration measurements in summer than spring and autumn.

The highest CO_2 uptake (GPP) occurs during summer, then spring, autumn and the lowest in winter. This is consistent with the fact that PAR values are higher in summer compared with the other seasons and are lower in winter.

PM3 showed higher GPP than the other four sites and PM1 was the lowest. This suggests that plant composition in PM3 are more productive than the other sites.

Regarding the NEE for the four sites, PM3 indicated CO_2 uptake during the four seasons, while the other three sites indicated CO_2 release. PM1 was the lowest CO_2 release fluxes during four seasons. This leaves PM2 & PM4 as the major sources of CO_2 in the study sites.

4.3.3 Plant Composition

The results reveal that PM2 & PM4 are having the highest soil respiration rates (even at the low temperatures); and PM1 & PM3 the lowest in respiration and very low at low temperature levels. Also, PM3 demonstrates highest primary production and PM1 the lowest.

Comparing modelled respiration fluxes of PM2 and PM4 show that respiration seasonal fluxes are almost the same in both sites. Considering that study sites PM4 and PM2 feature the same plant composition with larger *Pinus mugo* individuals at PM4 indicate the low impact of aboveground biomass size on respiration therefore respiration is much affected by belowground activities. Taking into account the low impact of water table variability as discussed above, leaves the temperature as a controlling factor affecting respiration process.

On the contrary to soil respiration, PM2 and PM4 modelled production fluxes of PM2 and PM4, show that PM4 has higher production in summer than PM2 and also higher in production than PM2 in the other three seasons. As above, taking into consideration that study sites PM4 and PM2 having the same plant composition with larger *Pinus mugo* individuals at PM4 indicate the impact of aboveground biomass size on production (the larger the mass the larger the area subjected to PAR leading to higher production fluxes) regardless of seasonal variability.

Low production and respiration fluxes modelled in PM1 (*Eriophorum vaginatum & Rhynchospora alba*) could be explained by considering the low aboveground biomass density in PM1, which is in line with the above comparison between PM2 & PM4. Likewise, the low R_{eco} is resulting from the low aboveground biomass density and consequently the less dead plants available for decomposition. (M. Minke et al, 2015) results presented similar conclusion for *Eriophorum–Carex*, showing the lowest production and respiration annual fluxes among the study vegetation compositions. As per (The Plant List version 1.1, 2013), both vegetation composition (*Eriophorum vaginatum & Rhynchospora alba and Eriophorum–Carex*) are under the same family "*Cyperaceae*" of the major group *Angiosperms* (Flowering plants).

PM3 plants composition (*Calluna vulgaris*) has the highest production as well as low respiration rates. Suggesting that the plants composition at this site "PM3" could be more decomposition resistant and also more productive than the other three plants composition, even at the high summer temperature and draught or at the low winter temperature and less water availability. This was discussed by (Wallèn, 1987), as *Calluna vulgaris* has good survival mechanism by the ability of renew its roots resulting to a higher underground biomass than the aboveground biomass, the percentage of the aboveground biomass to the total biomass varied between 35%-50% (Wallèn, 1987).

This suggest that the decomposition rates of PM2 & PM4 (*Pinus mugo*) are higher than at PM1 & PM3 and the plants litter are more vulnerable to microbial activities even at low temperatures.

The low difference between GPP and R_{eco} in PM1 (NEE), suggests that PM1 (*Eriophorum vaginatum & Rhynchospora alba*) is not a major contributor to the peat status since the resulting NEE is not significant compared to the resulting NEE at the other three sites. The more abundance of PM3 (*Calluna vulgaris*) will increase CO_2 storage in the study area, while the more abundance of PM2 & PM4 (*Pinus mugo*) will increase CO_2 release from the study area. This result, with regard to PM1, is supported by the assumption of (Petra Straková et al, 2012) that ombrotrophic graminoids and thicker (2-10 mm) tree roots (*E. vaginatum*) has the lowest mass loss rate (lowest respiration). On the other hand, this is not supported for the other sites, as the assumption says that minerotrophic graminoids (*Calluna*) has higher mass loss rate than fine roots (< 2 mm) of trees and shrubs (*Pinus*). Having the lowest water table at PM3 among the study sites would not also explain such difference specially the results are showing low dependency on water table variability. Therefore, nutrients availability and microbial community might explain this difference in assumptions.

The above discussion confirms that plant composition regulates CO_2 cycling as discussed by (A. Armstrong et at, 2015) and particularly plants' growth rate. Also, (M. Minke et al, 2015) concluded that vegetation biomass including the role of vegetation composition and species provides the best explanation of CO_2 annual balance.

This is in line with (Manuel Acosta et al, 2017) discussion which, showed how vegetation composition have a significant role in the peatland status and is an influencing parameter. Since, one of the adjacent plant communities may act as a CO_2 sink while, simultaneously, another is a source. This plant composition affects the CO_2 exchange status on seasonal scale more than on the daily scale since plants have different seasonal growing patterns affecting the above and below ground biomass (Manuel Acosta et al, 2017).

CHAPTER 5 - CONCLUSIONS

CO_2 exchanges between the atmosphere and four typical plant compositions of a peat bog (located in Püergschachen Moor in the Styrian Enns valley, Austria) fluxes were measured (which represent four typical different plant compositions of the study area). Measurements were conducted during spring, summer and autumn using the closed dynamic chamber approach. CO_2 measurements were implemented using an infrared gas analyser. The seasonal variability and diurnal variations of ecosystem respiration (R_{eco}), gross primary production (GPP) and net ecosystem exchange (NEE) were investigated with respect to photosynthetic active radiation (PAR) and soil temperature measured at 2 cm depth and water table depths. Finally, production and respiration were modelled in order to provide fluxes covering the whole year and to calculate the total CO_2 exchange for the ecosystem during the respective measurement seasons. In the model, R_{eco} is estimated based on temperature correlation and NEE based on PAR correlation. GPP was calculated from the balance between NEE and R_{eco}.

In the course of a day, results show that NEE at lowest PAR values <100 µmol photon^{-1} m^{-2} s^{-1} indicating CO_2 release and suggesting low production (GPP) processes; then GPP starts to increase with PAR resulting in higher CO_2 uptake rates. PAR was not the only factor affecting GPP, temperature plays a role as well. Warmer seasons are showing higher production fluxes as a result of the longer growing seasons than colder seasons. Results also show that respiration is directly related to temperature variability. On the other hand, respiration revealed low dependency on water table changes. This could be due to less significant level changes during measurement periods or as a result of soil water retention characteristics.

The total modelled annual production and respiration showed different behaviour patterns between the four sites and the seasons, suggesting that plant composition affects biomass production and soil respiration processes. This could result from different characteristics of plants regarding photoactivity, biomass production, size, seasonal development stages and interaction with climatic conditions such as temperature and solar irradiation.

The model show that highest annual GPP was at PM3 (-3.854 kg m^{-2} y^{-1}) and the lowest was at PM1 (-2.209 kg m^{-2} y^{-1}) and the highest respiration was PM2 (3.761 kg m^{-2} y^{-1}) and the lowest was PM1 (2.463 kg m^{-2} y^{-1}). NEE results demonstrate that PM3 (-1.129 kg m^{-2} y^{-1}) represents highest CO_2 sink and PM2 (1.227 kg m^{-2} y^{-1}) highest CO_2 source.

The high respiration fluxes at PM2 & PM4 indicate that the decomposition rates of (*Pinus mugo*) are high and the organic matter/litter are labile for microbial activities even at low temperatures. The difference in size between PM2 & PM4 plants composition affected the primary production (PM4 has higher production fluxes than PM2) rather the respiration fluxes.

PM3 plants composition (*Calluna vulgaris*) is more resistant to decomposition and more productive than the other three plants composition, even at the high summer temperature and drought or at the low winter temperature with low water availability.

PM1 plants composition (*Eriophorum vaginatum & Rhynchospora alba*) is not decomposed easily but has low production rate at the same time leading to low NEE compared with the other three plant compositions.

The low difference between GPP and R_{eco} in PM1 (NEE), suggests that PM1 (*Eriophorum vaginatum & Rhynchospora alba*) is not a major contributor to the peat status since the resulting NEE is not significant compared to the resulting NEE in the other three sites. The more abundance of PM3 (*Calluna vulgaris*) will increase CO_2 storage in the study area, while the more abundance of PM2 & PM4 (*Pinus mugo*) will increase CO_2 release from the study area. This confirms the significant role of vegetation composition in the peatland constituting an influencing parameter in carbon exchange within this ecosystem, and affecting its status as a CO_2 sink or source.

REFERENCES

A. Armstrong et at. (2015). Biotic and Abiotic Factors Interact to Regulate Northern Peatland Carbon Cycling.

Bogdan H. Chojnicki et al. (2009). *Measurements of Carbon Dioxide Fluxes by Chamber Method at the Rzecin Wetland Ecosystem, Poland.* Poland: Polish J. of Environ. Stud. Vol. 19, No. 2 (2010), 283-291.

F. St-Hilaire et al. (2010). *McGill wetland model: evaluation of a peatland carbon simulator.* Canada: Biogeosciences.

F.J.W. Parmentier et al. (2008). *CO2 fluxes and evaporation on a peatland in the Netherlands appear not affected by water table fluctuations.* The Netherlands: Elsevier.

Frolking S. et al. (2011). Peatlands in the Earth's 21st century climate system.

G. Burba et al. (2010). *Introduction to the Eddy Covariance Method.* LI-COR Biosciences.

H. Biester et al. (2014). *Comparison of different methods to determine the degree of peat decomposition in peat bogs.* Germany: Biogeosciences.

Joosten et al. (2002). *Wise Use of Mires and Peatlands.* UK: International Mire Conservation Group and International Peat Society.

Jurasinski et al, G. (2014). *Flux rate calculation from dynamic closed chamber measurements - Package 'flux'.* Germany.

Kasimir et al. (1997). *Greenhouse gas emissions from farmed organic soils.*

L. Kutzbach et al. (2007). *CO2 flux determination by closed-chamber methods can be seriously biased by inappropriate application of linear regression.* Germany: Biogeosciences.

Lindsay, R. (2010). Peat accumulation and decomposition. In R. Lindsay, *Peatbogs and carbon, a critical synthesis* (p. Chapter 7). UK: Environmental Research Group - University of London.

M. Litvak. (2007, February 22). Evaporation from Flux Towers. University of New Mexico.

M. Minke et al. (2015). Water level, vegetation composition and plant productivity explain greenhouse gas fluxes in temperate cutover fens after inundation.

M. Schumann et al. (2008). *Global Peatland Restoration Manual.* Germany: Institute of Botany and Landscape Ecology, Greifswald University.

Manuel Acosta et al. (2017). CO2 Fluxes from Different Vegetation Communities on a Peatland Ecosystem.

O. Koch et al. (2008). Interannual Ecosystem CO2 Dynamics in Alpine Zone of the Eastern Alps, Austria.

P. C. Stoy et al. (2013). *Evaluating the agreement between measurements and models of net ecosystem exchange at different times and timescales using wavelet coherence: an example using data from the North American Carbon Program Site-Level Interim Synthesis.* USA: Biogeosciences.

Petra Straková et al. (2012). Disentangling direct and indirect effects of water table drawdown on above- and belowground plant litter decomposition:Consequences for accumulation of organic matter in boreal peatlands.

S. Beetz et al. (2013). *Effects of land use intensity on the full greenhouse gas balance in an Atlantic peat bog.* Germany.

S. Glatzel et al. (2016, October 7). *Pürgschachen Moor - Austria*. Retrieved from DEIMS, the (Drupal Ecological Information Management System): https://data.lter-europe.net/deims/site/e493935a-0e70-4a15-bb5b-023573c5bdd8

Spilatro, S. R. (1998). *Preparing a photosynthesis light response curve*. Retrieved from Department of Biology, Marrieta College, Marietta, Ohio: http://w3.marietta.edu/~spilatrs/biol103/photolab/photosyn.html

Strack M. et al. (2008). Northern Peatlands, Greenhouse Gas Exchange and Climate Change. In M. Strack, *Peatlands and Climate Change* (p. Chapter 2). International Peat Socity.

The Plant List version 1.1. (2013, September). Retrieved from The Plant List : http://www.theplantlist.org/

Wallèn, B. (1987). Growth Pattern and Distribution of Biomass of Calluna vulgaris on an Ombrotrophic Peat Bog.

Zerva, A. (2004). *Comparison of closed static and dynamic chamber methods for the measurement of soil CO2 efflux.*

I have endeavored to provide all the holders of the mage rights and seek their consent to use the images in this Work. Should a copyright infringement become known, I request Message with me.

ANNEXES

Annex 1 – CO_2 Fluxes Calculations' *R*-Script

```
# ***************************************************************
# ******** G.E.R.D (Gas Emission Research Detector) ***************
# ***************************************************************

# ********************** NOTES: this script *********************
# This script runs in four (4) steps:
        #STEP 1: making single measurement files
        #STEP 2: TIME DIFFERENCE
        #STEP 3: FLUX CALCULATIONS
        #STEP 4: Merging all Fluxes in one
# This approach will help to detect which measurement has a problem during
# flux calculations.
# Steps 1 & 2 can run together, then Step 3 need to run alone and finally Step 4 runs.
# In Step 3, measurement with successful flux is deleted from the folder. When we have
# a measurement with no success calculations, the script stops and we can go to the
# folder "a02_output_data_tmp_time" and we can isolate the relevant measurement.

# We need to create six (6) folders:
# "00_input_data" - "01_output_data" - "02_output_data_Archive_time"
# "a01_output_data_tmp" - "a02_output_data_tmp_time" - "a03_output_data_tmp_flux"
# setwd => must be adjusted.

# "input_data" folder => will contain the data received

# Before each run of the script:
# 1) The temporary folders "_tmp" must be empty.
# 2) The "input_data" folder should contain only the required input files.
#    Any extra files must be deleted.
# 3) The output file name => must be defined inside the script

# Flux calculations in this script done by using "Package 'Flux' - February 19,2015"
# Title "Flux rate calculation from dynamic closed chamber measurements"
# Version 0.3-0 - Date 2014-04-23
# Author Gerald Jurasinski, Franziska Koebsch, Anke Guenther, Sascha Beetz

# The following packages need to installed:
#install.packages("caTools")
#install.packages("flux")

# CO2 flux is measured in "g per sq.m per hr"
# ***************************************************************

#==================================== START ===================================
```

```
#==============================================================================
#================= STEP 1: making single measurement files ==================
#==============================================================================

rm(list = ls())
setwd("D:/Asaad/R-work/00_input_data/")

range_lim <- 1  # VIP (very important parameter)

#====================== ADDING FILES TOGETHER ==========================

file_list <- list.files()

# reading each data file and adding them together
for (file in file_list){

  # if the merged dataset doesn't exist, create it
  if (!exists("gcc_tmp")){
    gcc_tmp <- read.table(file, sep=";", stringsAsFactors = FALSE)
  }

  # if the merged dataset does exist, append to it
  if (exists("gcc_tmp")){
    temp_dataset <-read.table(file, sep=";", stringsAsFactors = FALSE)
    colnames(temp_dataset) <- colnames(gcc_tmp)
    gcc_tmp<-rbind(gcc_tmp, temp_dataset)
    rm(temp_dataset)
  }

}

gcc_tmp["time_diff"] <- NA
gcc_tmp["time_format"] <- NA

## baptize the columns:
colnames(gcc_tmp) <- c("Date", "Time", "SessionNr", "RecordNr",
                "Site", "CO2ppm", "Pump_Pre", "Pump_Temp",
                "PAR", "Chamb_Temp", "Air_Temp", "Soil_Temp_2",
                "Soil_Temp_5", "Soil_Temp_10", "Bat-Volt",
                "Chamb_Area", "Chamb_Height", "HK", "Transp_Opaque",
                "time_diff", "time_format")

#write.table(gcc_tmp, "F:/R_files/01_output_data/2016-03-18XX.txt", sep =";")

#====================== FIXING CHAMBER HEIGHT ===========================

gcc_tmp$Chamb_Height<-ifelse(gcc_tmp$Site=='PM04-3',1.07,0.535)

gcc_tmp["Chamb_Vol"] <- NA
```

```
gcc_tmp$Chamb_Vol<-gcc_tmp$Chamb_Area * gcc_tmp$Chamb_Height


# date in these steps is the current date. But since we are comparing time within the same
# day, the day could be neglected

gcc_tmp$time_format<-strptime(gcc_tmp$Time, "%H:%M:%S")

#write.table(gcc, "F:/R_files/01_output_data/2016-03-18.txt", sep =";")

# Splitting the data frame to separate data frames per each chamber measurement

g <- split(gcc_tmp, gcc_tmp$SessionNr)

# Each data frame is saved in a separate file in the "output_data_tmp" folder

setwd("D:/Asaad/R-work/a01_output_data_tmp/")

for (i in seq_along(g)) {

  write.table(g[[i]], paste(names(g)[i], ".txt", sep = ""), row.names = FALSE, sep =";")
}

#==============================================================================
#===================== STEP 2: TIME DIFFERENCE ==========================
#==============================================================================

# read the files to calculate the time difference and save again

setwd("D:/Asaad/R-work/a01_output_data_tmp/")

file_list <- list.files()

for (file in file_list)
  {
  setwd("D:/Asaad/R-work/a01_output_data_tmp/")

    gcc <- read.table(file, header = TRUE, sep=";", stringsAsFactors = FALSE)

   time1 <- gcc[1,"time_format"]

    m=500
    for(x in 1:m)
    {
      time2 <- gcc[,"time_format"]
      z <- difftime(time2, time1, units = c("secs")) # "mins"
      gcc$time_diff<- z
    }
```

```
  setwd("D:/Asaad/R-work/a02_output_data_tmp_time/")

  L <- gcc$SessionNr[1]
  write.table(gcc, file=paste(L, ".txt", sep = ""), row.names = FALSE, sep =";")
  rm(gcc)
}


file.copy("D:/Asaad/R-work/a02_output_data_tmp_time/.","D:/Asaad/R-
work/02_output_data_Archive_time/.", recursive = T)


#================================================================================
#======================= STEP 3: FLUX CALCULATIONS ========================
#================================================================================

library(caTools)
library(flux)


# read the files to calculate and the flux per measurement

setwd("D:/Asaad/R-work/a02_output_data_tmp_time/")

file_list <- list.files()

for (file in file_list)
 {

   gcc <- read.table(file, header = TRUE, sep=";", stringsAsFactors = FALSE)

   ## Create dataframes per chamber measurement:
   gcc.parts <- chop(gcc, factors = c("Site", "Date", "SessionNr"), nmes=
                     c("Site", "Date" ,"SessionNr"),min.cm = 3)

    vp.CO2 <- list(CO2 = "CO2ppm", time = "time_diff", CO2.gcq = 0.0, volume = "Chamb_Vol",
           t.air = "Air_Temp", area = "Chamb_Area", p.air = 101325)

   flux.CO2 <- fluxx(gcc.parts,  var.par = vp.CO2, min.dp = 5,
             range.lim=3, out.unit="g",
            loop = "auto") # changing: min.dp=5 / rang.lim=3


   k <- gcc$SessionNr[1]
   setwd("D:/Asaad/R-work/a03_output_data_tmp_flux/")
   export(flux.CO2, file=paste(k, "-flux.txt", sep = ""))

   rm(gcc)
   setwd("D:/Asaad/R-work/a02_output_data_tmp_time/")
```

```
  file.remove(file)

 }


#===============================================================================
#===================== STEP 4: Merging all Fluxes in one ======================
#===============================================================================

rm(list = ls())
setwd("D:/Asaad/R-work/a03_output_data_tmp_flux/")

file_list <- list.files()

# reading each data file and adding them together
for (file in file_list){

 # if the merged dataset doesn't exist, create it
 if (!exists("flux_tmp")){
  flux_tmp <- read.table(file, sep=" ", stringsAsFactors = FALSE)
 }

 # if the merged dataset does exist, append to it
 if (exists("flux_tmp")){
  temp_dataset <-read.table(file, sep=" ", stringsAsFactors = FALSE)
  colnames(temp_dataset) <- colnames(flux_tmp)
  flux_tmp<-rbind(flux_tmp, temp_dataset)
  rm(temp_dataset)
 }

}

write.table(flux_tmp, "D:/Asaad/R-work/01_output_data/2015-Full_Year_CO2.txt", sep =";")
```

Annex 2 – Sites' Frames Results

	Season	Frame	GPP	R_{eco}	NEE
Site PM1	Spring	PM1-1	-0.550	0.316	-0.234
		PM1-2	-0.616	0.357	-0.259
		PM1-3	-0.469	0.274	-0.195
	Summer	PM1-1	-1.668	0.848	-0.820
		PM1-2	-0.980	0.689	-0.291
		PM1-3	-1.446	0.839	-0.607
	Autumn	PM1-1	-0.252	0.105	-0.147
		PM1-2	-0.353	0.126	-0.227
		PM1-3	-0.312	0.117	-0.195
Site PM2	Spring	PM2-1	-0.846	0.341	-0.505
		PM2-2	-0.807	0.301	-0.505
		PM2-3	-0.666	0.361	-0.305
	Summer	PM2-1	-1.053	0.855	-0.198
		PM2-2	-0.971	0.761	-0.210
		PM2-3	-1.068	0.762	-0.305
	Autumn	PM2-1	-0.577	0.467	-0.110
		PM2-2	-0.232	0.111	-0.121
		PM2-3	-0.459	0.334	-0.125
Site PM3	Spring	PM3-1	-0.859	0.339	-0.521
		PM3-2	-0.783	0.281	-0.501
		PM3-3	-0.627	0.365	-0.262
	Summer	PM3-1	-1.526	0.731	-0.795
		PM3-2	-1.743	0.806	-0.937
		PM3-3	-1.353	0.618	-0.735
	Autumn	PM3-1	-0.393	0.168	-0.226
		PM3-2	-0.366	0.118	-0.247
		PM3-3	-0.526	0.254	-0.272
Site PM4	Spring	PM4-1	-0.445	0.317	-0.128
		PM4-2	-0.647	0.365	-0.282
		PM1-3	-0.843	0.444	-0.399
	Summer	PM4-1	-1.075	0.957	-0.118
		PM4-2	-1.281	0.745	-0.535
		PM4-3	-1.393	0.728	-0.665
	Autumn	PM4-1	-0.811	0.774	-0.037
		PM4-2	-0.373	0.111	-0.262
		PM4-3	-0.345	0.139	-0.206

Table 30: Average seasonal NEE, day time R_{eco} and calculated GPP per Frame

Annex 3 – NEE and R_{eco} Models

Hours	Soil Temp. at 2cm (°C)				PAR (μmol photon^{-1} m^{-2} s^{-1})			
	Spring	Summer	Autumn	Winter	Spring	Summer	Autumn	Winter
5:00	10.207	15.122	8.641	2.484		16.406		
6:00	10.27	15.25	8.57	2.42	87.18	115.12	10.96	
7:00	11.32	15.80	8.70	2.34	277.72	331.17	69.86	0.40
8:00	12.61	16.62	9.02	2.49	426.73	597.51	174.35	20.71
9:00	14.17	17.84	9.59	2.42	595.02	860.17	304.84	60.36
10:00	15.53	19.68	10.42	2.69	797.62	1079.72	484.99	116.32
11:00	16.46	22.08	11.42	2.47	879.53	1205.06	604.47	190.27
12:00	17.79	24.12	12.43	2.73	966.12	1264.15	647.29	381.22
13:00	18.51	25.62	13.13	2.74	938.23	1267.48	598.28	393.14
14:00	18.73	26.39	13.32	3.42	849.82	1133.33	496.34	307.59
15:00	18.42	26.24	13.12	3.20	703.09	967.29	349.98	154.27
16:00	17.97	25.47	12.67	2.81	558.97	761.93	185.09	23.79
17:00	17.33	24.22	12.01	2.43	389.58	502.36	57.62	0.16
18:00	16.34	22.66	11.21	2.30	231.00	275.08	7.60	
19:00	15.32	21.15	10.56	2.37	83.06	96.59		
20:00	14.21	19.86	10.14	2.38		10.96		
21:00	13.24	18.77	9.80	2.32		0.57		
22:00	12.57	17.95	9.51	2.31				
23:00	12.18	17.30	9.27	2.29				
0:00	11.73	16.71	9.18	2.26				
1:00	11.25	16.28	9.04	2.21				
2:00	10.88	15.94	8.92	2.26				
3:00	10.62	15.62	8.82	2.44				
4:00	10.42	15.33	8.72	2.54				

(shaded) Indicates day time hours

Table 31: Average recorded measurements "from Eddy measurement station"

Hours	Spring				Summer			
	PM1	PM2	PM3	PM4	PM1	PM2	PM3	PM4
5:00					-0.299	-0.337	-0.607	-0.491
6:00	-0.146	-0.253	-0.499	-0.381	-0.344	-0.387	-0.658	-0.532
7:00	-0.262	-0.369	-0.620	-0.484	-0.450	-0.504	-0.777	-0.630
8:00	-0.369	-0.472	-0.729	-0.577	-0.587	-0.652	-0.928	-0.755
9:00	-0.494	-0.591	-0.855	-0.685	-0.737	-0.807	-1.089	-0.889
10:00	-0.625	-0.721	-0.991	-0.800	-0.893	-0.957	-1.247	-1.025
11:00	-0.693	-0.783	-1.058	-0.858	-1.032	-1.076	-1.377	-1.140
12:00	-0.777	-0.857	-1.138	-0.928	-1.132	-1.154	-1.465	-1.220
13:00	-0.793	-0.861	-1.146	-0.938	-1.189	-1.192	-1.511	-1.263
14:00	-0.766	-0.824	-1.110	-0.910	-1.164	-1.146	-1.470	-1.234
15:00	-0.696	-0.746	-1.031	-0.846	-1.093	-1.063	-1.386	-1.166
16:00	-0.622	-0.666	-0.949	-0.778	-0.982	-0.946	-1.266	-1.066
17:00	-0.530	-0.569	-0.850	-0.695	-0.832	-0.791	-1.106	-0.932
18:00	-0.430	-0.469	-0.745	-0.607	-0.684	-0.644	-0.952	-0.802
19:00	-0.333	-0.374	-0.645	-0.522	-0.556	-0.522	-0.822	-0.691
20:00					-0.474	-0.450	-0.744	-0.622
21:00					-0.429	-0.418	-0.707	-0.587
22:00								
23:00								
0:00								
1:00								
2:00								
3:00								
4:00								

Hours	Autumn				Winter			
	PM1	PM2	PM3	PM4	PM1	PM2	PM3	PM4
5:00								
6:00	-0.053	-0.175	-0.413	-0.305				
7:00	-0.081	-0.206	-0.444	-0.330		-0.018	-0.225	-0.125
8:00	-0.135	-0.264	-0.504	-0.379		-0.031	-0.239	-0.137
9:00	-0.208	-0.340	-0.582	-0.445		-0.049	-0.256	-0.150
10:00	-0.310	-0.447	-0.692	-0.537		-0.082	-0.290	-0.179
11:00	-0.395	-0.528	-0.779	-0.611		-0.112	-0.319	-0.201
12:00	-0.450	-0.573	-0.829	-0.656	-0.056	-0.210	-0.418	-0.281
13:00	-0.457	-0.567	-0.826	-0.657	-0.061	-0.216	-0.424	-0.286
14:00	-0.423	-0.523	-0.783	-0.623	-0.027	-0.191	-0.403	-0.273
15:00	-0.357	-0.448	-0.707	-0.562		-0.112	-0.323	-0.208
16:00	-0.275	-0.358	-0.616	-0.486		-0.040	-0.250	-0.147
17:00	-0.200	-0.281	-0.536	-0.419		-0.020	-0.227	-0.128
18:00	-0.150	-0.237	-0.488	-0.377				
19:00								

Hours	Autumn				Winter			
	PM1	PM2	PM3	PM4	PM1	PM2	PM3	PM4
20:00								
21:00								
22:00								
23:00								
0:00								
1:00								
2:00								
3:00								
4:00								
	Indicates day time hours							

Table 32: Hourly seasonal GPP estimate (g m^{-2} h^{-1})

Hours	Spring				Summer			
	PM1	PM2	PM3	PM4	PM1	PM2	PM3	PM4
5:00					0.089	0.176	-0.196	0.021
6:00	0.061	0.142	-0.230	-0.006	0.050	0.128	-0.243	-0.017
7:00	-0.015	0.051	-0.320	-0.079	-0.036	0.025	-0.346	-0.099
8:00	-0.074	-0.021	-0.391	-0.136	-0.142	-0.103	-0.473	-0.201
9:00	-0.141	-0.101	-0.472	-0.200	-0.247	-0.228	-0.598	-0.301
10:00	-0.222	-0.198	-0.568	-0.277	-0.334	-0.333	-0.702	-0.385
11:00	-0.255	-0.238	-0.607	-0.309	-0.384	-0.394	-0.762	-0.433
12:00	-0.289	-0.279	-0.648	-0.342	-0.408	-0.422	-0.790	-0.455
13:00	-0.278	-0.266	-0.635	-0.331	-0.409	-0.423	-0.792	-0.457
14:00	-0.243	-0.223	-0.593	-0.297	-0.356	-0.359	-0.728	-0.405
15:00	-0.184	-0.153	-0.523	-0.241	-0.289	-0.280	-0.649	-0.342
16:00	-0.127	-0.084	-0.454	-0.186	-0.208	-0.181	-0.551	-0.264
17:00	-0.060	-0.003	-0.374	-0.122	-0.104	-0.057	-0.427	-0.165
18:00	0.004	0.073	-0.298	-0.061	-0.014	0.052	-0.319	-0.078
19:00	0.062	0.144	-0.228	-0.005	0.057	0.137	-0.234	-0.010
20:00					0.091	0.178	-0.193	0.023
21:00					0.095	0.183	-0.188	0.027
22:00								
23:00								
0:00								
1:00								
2:00								
3:00								
4:00								

Hours	Autumn				Winter			
	PM1	PM2	PM3	PM4	PM1	PM2	PM3	PM4
5:00								
6:00	0.091	0.178	-0.193	0.023				
7:00	0.068	0.150	-0.221	0.000	0.095	0.183	-0.188	0.027
8:00	0.026	0.100	-0.271	-0.040	0.087	0.174	-0.198	0.019
9:00	-0.026	0.038	-0.333	-0.089	0.072	0.155	-0.217	0.004
10:00	-0.097	-0.049	-0.419	-0.158	0.049	0.128	-0.244	-0.017
11:00	-0.145	-0.106	-0.476	-0.204	0.020	0.092	-0.279	-0.046
12:00	-0.162	-0.126	-0.497	-0.220	-0.056	0.001	-0.370	-0.119
13:00	-0.143	-0.103	-0.473	-0.201	-0.061	-0.005	-0.375	-0.123
14:00	-0.102	-0.054	-0.425	-0.162	-0.027	0.036	-0.335	-0.090
15:00	-0.044	0.016	-0.355	-0.107	0.034	0.110	-0.262	-0.032
16:00	0.022	0.095	-0.276	-0.044	0.086	0.172	-0.200	0.018
17:00	0.073	0.156	-0.216	0.005	0.095	0.184	-0.188	0.027
18:00	0.093	0.180	-0.192	0.024				

Hours	Autumn				Winter			
	PM1	PM2	PM3	PM4	PM1	PM2	PM3	PM4
19:00								
20:00								
21:00								
22:00								
23:00								
0:00								
1:00								
2:00								
3:00								
4:00								

Indicates day time hours

Table 33: Hourly seasonal day time NEE estimate (g m^{-2} h^{-1})

Hours	Spring				Summer			
	PM1	PM2	PM3	PM4	PM1	PM2	PM3	PM4
5:00	0.205	0.393	0.267	0.373	0.388	0.513	0.411	0.511
6:00	0.207	0.394	0.269	0.375	0.393	0.516	0.415	0.515
7:00	0.247	0.420	0.300	0.405	0.414	0.529	0.431	0.531
8:00	0.295	0.451	0.338	0.441	0.444	0.549	0.455	0.554
9:00	0.353	0.489	0.383	0.485	0.490	0.579	0.491	0.588
10:00	0.403	0.522	0.423	0.523	0.558	0.624	0.545	0.640
11:00	0.438	0.545	0.450	0.549	0.648	0.682	0.615	0.707
12:00	0.488	0.578	0.489	0.586	0.724	0.732	0.675	0.764
13:00	0.515	0.595	0.511	0.607	0.780	0.768	0.719	0.807
14:00	0.523	0.600	0.517	0.613	0.809	0.787	0.742	0.828
15:00	0.511	0.593	0.508	0.604	0.803	0.783	0.737	0.824
16:00	0.495	0.582	0.495	0.592	0.775	0.765	0.715	0.802
17:00	0.471	0.566	0.476	0.574	0.728	0.734	0.678	0.767
18:00	0.434	0.542	0.447	0.546	0.670	0.696	0.632	0.724
19:00	0.396	0.517	0.417	0.517	0.614	0.660	0.588	0.681
20:00	0.354	0.490	0.384	0.486	0.565	0.628	0.550	0.645
21:00	0.318	0.467	0.356	0.459	0.525	0.601	0.518	0.614
22:00	0.293	0.450	0.336	0.440	0.494	0.582	0.494	0.591
23:00	0.279	0.441	0.325	0.429	0.470	0.566	0.475	0.573
0:00	0.262	0.430	0.312	0.416	0.448	0.551	0.458	0.556
1:00	0.244	0.418	0.298	0.403	0.432	0.541	0.445	0.544
2:00	0.230	0.409	0.287	0.392	0.419	0.533	0.435	0.535
3:00	0.220	0.403	0.279	0.385	0.407	0.525	0.426	0.525
4:00	0.213	0.398	0.273	0.379	0.396	0.518	0.417	0.517

Hours	Autumn				Winter			
	PM1	PM2	PM3	PM4	PM1	PM2	PM3	PM4
5:00	0.146	0.355	0.221	0.329		0.205	0.041	0.156
6:00	0.144	0.353	0.219	0.327		0.203	0.039	0.154
7:00	0.149	0.356	0.223	0.331		0.201	0.037	0.152
8:00	0.161	0.364	0.232	0.340		0.205	0.041	0.156
9:00	0.182	0.378	0.249	0.356		0.203	0.039	0.154
10:00	0.213	0.398	0.273	0.379		0.210	0.047	0.162
11:00	0.250	0.422	0.303	0.407		0.204	0.040	0.155
12:00	0.288	0.447	0.332	0.436		0.211	0.048	0.163
13:00	0.314	0.464	0.353	0.456		0.211	0.048	0.163
14:00	0.321	0.469	0.358	0.461		0.227	0.068	0.182
15:00	0.314	0.464	0.353	0.455		0.222	0.062	0.176
16:00	0.297	0.453	0.339	0.442		0.213	0.050	0.165
17:00	0.272	0.437	0.320	0.424		0.203	0.039	0.155
18:00	0.242	0.417	0.297	0.401		0.200	0.035	0.151

Hours	Autumn				Winter			
	PM1	PM2	PM3	PM4	PM1	PM2	PM3	PM4
19:00	0.218	0.401	0.277	0.383		0.202	0.037	0.153
20:00	0.202	0.391	0.265	0.371		0.202	0.037	0.153
21:00	0.190	0.383	0.255	0.362		0.201	0.036	0.151
22:00	0.179	0.376	0.247	0.354		0.200	0.036	0.151
23:00	0.170	0.370	0.240	0.347		0.200	0.035	0.150
0:00	0.167	0.368	0.237	0.344		0.199	0.034	0.150
1:00	0.161	0.364	0.233	0.340		0.198	0.033	0.148
2:00	0.157	0.362	0.229	0.337		0.199	0.034	0.150
3:00	0.153	0.359	0.226	0.334		0.204	0.039	0.155
4:00	0.149	0.357	0.223	0.331		0.206	0.042	0.157

Indicates day time hours

Table 34: Hourly seasonal R_{eco} estimate (g m^{-2} h^{-1})